

See discussions, stats, and author profiles for this publication at: <https://www.researchgate.net/publication/260252232>

Nonlinear Model Predictive Control approach in design of Adaptive Cruise Control with automated switching to cruise control

Article in *Control Engineering Practice* · May 2014

DOI: 10.1016/j.conengprac.2014.01.016

CITATIONS

71

READS

2,420

2 authors:



Payman Shakouri

Ford Motor Company, Dunton Technical Centre, United Kingdom

12 PUBLICATIONS 311 CITATIONS

[SEE PROFILE](#)



A. Ordys

Warsaw University of Technology

166 PUBLICATIONS 1,568 CITATIONS

[SEE PROFILE](#)

Some of the authors of this publication are also working on these related projects:



Special Issue "Cogeneration Systems: Measurements, Data Analysis, Modelling and Control" in Applied Sciences IF=2.217 [View project](#)



Designing of the adaptive cruise control system-switching controller [View project](#)



Nonlinear Model Predictive Control approach in design of Adaptive Cruise Control with automated switching to cruise control



Payman Shakouri*, Andrzej Ordys

School of Mechanical and Automotive Engineering, Kingston University London, Friars Avenue, Roehampton Vale, London SW15 3DW, UK

ARTICLE INFO

Article history:

Received 15 July 2011

Accepted 17 January 2014

Available online 17 February 2014

Keywords:

Vehicle dynamic

Adaptive Cruise Control

Model Predictive Control

Nonlinear Model Predictive Control

State-dependent linear model

ABSTRACT

In this paper the Nonlinear Model Predictive Control (NMPC) is used in designing of Adaptive Cruise Control (ACC) and Cruise Control (CC) systems. An algorithm is proposed to carry out automatic switching between ACC and CC, depending on the situation in front of the vehicle. Also, an algorithm based on MPC equation is devised to obtain the prediction of future reference trajectories corresponding to desired speed and distance. NMPC equation used in this paper is developed based on state-dependent representation of linear models corresponding to the modes of the operation: accelerating-throttle is active and braking-brake is active. The developed automated ACC system is tested in simulation against different scenarios proving good performance of the system. Furthermore, the results of proposed control algorithm based on NMPC methods are compared with a different ACC structure.

© 2014 Elsevier Ltd. All rights reserved.

1. Introduction

Adaptive Cruise Control (ACC) is an extension of the Cruise Control (CC) system which is capable of adjusting the velocity of the vehicle depending on the behaviour of other vehicles moving in front, by applying the brake and modulating the throttle to produce the necessary power (Xiao & Gao, 2010). This system uses the radar or other sensory devices to measure the distance between vehicles (Moon, Moon, & Yi, 2009; Winner, Winter, & Lucas, 2003). The extended version of the ACC is so-called ACC stop & go. Unlike the conventional ACC, which is unable to operate at speed below 30 km/h, the stop & go function, in combination with automatic transmission can operate at low speed and maintain the safe gap to the vehicle in front all the way down to standstill.

Along with the CC and ACC systems another version of the velocity controlling system has been introduced, so-called Look Ahead Cruise Controller (Hellström, Ivarsson, Åslund, & Nielsen, 2009; Kozica, 2005; Keulen et al., 2009). It uses the information about the road ahead of the vehicle to reduce the fuel consumption. For that purpose some “derivative velocity controlling system” is introduced, for instance; Predictive Cruise Control (PCC) (Lattemann, Neiss, Terwen, & Connolly, 2004), Expert Cruise Control (ECC) (Wingren, 2005) or Model Predictive control (MPC), (Axehill & Sjöberg, 2003).

It is known that ACC is capable of managing the traffic flow. By making platoons of vehicles it improves highway capacity. In ACC mode many vehicles can move at highway speed with small inter-distance which can increase density of the vehicles on the highway. It also has the positive effect on the optimisation of fuel consumption especially for heavy vehicles. This is due to significant effect of the aerodynamic drag dependent on the cross section front area for such vehicles (Vahidi & Eskandarian, 2003). On this matter, Cooperative Adaptive Cruise Control (CACC) has been proposed as an advance in the area of Intelligent Transportation Systems (ITS) – to increase traffic efficiency and to improve passenger comfort and safety (Desjardins & Chaib-draa, 2011; Shladover et al., 2009; ven Arem, ven Driel, & Visser, 2006; Ploeg, Serrarens, & Heijen, 2011). CACC requires that the distances between vehicles are controlled to a high precision and this in turn implies the use of direct communication – exchange of information between the vehicles in the platoon. This may be accomplished in two ways; Inter-Vehicle Communication (IVC) and Roadside-to-Vehicle Communication. IVC is conducted by exchanging information about congestion, incidents or emergency between the follower and leader vehicles through wireless communication. Other automotive safety system such as collision avoidance has also been incorporated in the vehicle to further assist the driver in enhancing safety and preventing accident with a sequence of warnings and active intervention (Isermann, Mannale, & Schmitt, 2012; Moon et al., 2009). Furthermore, since many automotive safety systems such as ACC, collision avoidance or emergency lane assist require accurate information about both road shape and object position, researches have been carried out on advancing the technologies applied for capturing those

* Corresponding author.

E-mail address: p.shakouri@kingston.ac.uk (P. Shakouri).

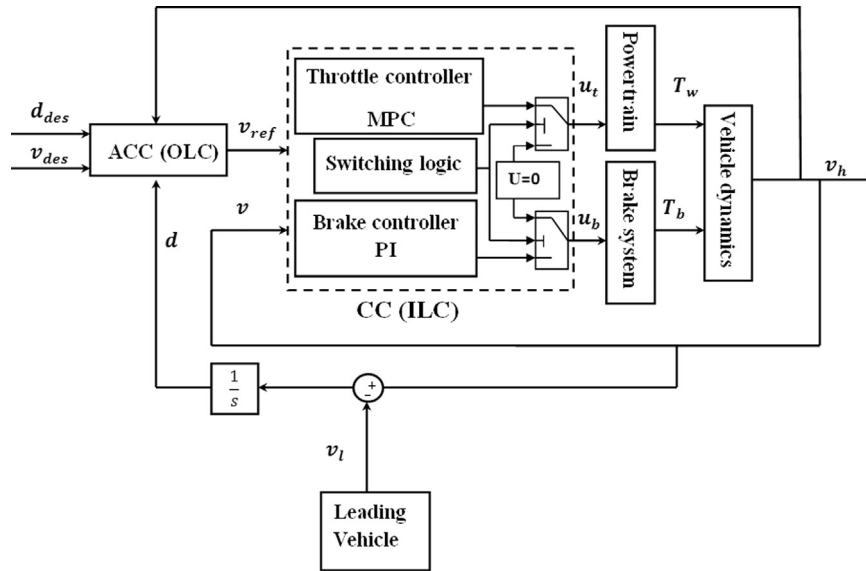


Fig. 1. The ACC structure based on two separate control loops; Outer-Loop Controller (OLC) and Inner-Loop Controller (ILC).

information (Park, Hwang, & Kang, 2010; Eidehall, Pohl, & Gustafsson, 2007; Matthews, An, & Harris, 1996).

The above approach relies on the availability of the IVC system. In this paper the assumption of such system availability is not made. However, improvements in control quality reported in this paper may have significance to situations being matter of interest for CACC approach – without the communication being available.

In literature, various control algorithms have been suggested considering the stop & go function. To design an ACC system being able to perform at the stop & go situation, (Martinez & Canudas-de-Wit, 2007) proposed a nonlinear reference model-based control approach with a compensator which uses a feedback loop so as to take the unmodeled and external disturbances into account. The considerable amount of work has been carried out in design of an ACC system through the model-based control design methods. An ACC structure is mainly developed consisting of two controller loops; outer loop controller and inner loop controller (see Fig. 1). The reason for introducing two levels of controller is to distinguish the vehicle dynamic control (brake and throttle control) design from highway control. Therefore, the outer loop controller can control the distance between vehicles regardless of the design of inner loop (which may be specific for a make/type of the vehicle). From this prospective, (Gerdes & Hedrick, 1997) designed a controller to accomplish the speed and distance tracking by utilising the multi-surface sliding controller consisting of three control levels. An additional level was introduced beside of two others mentioned levels, i.e. outer-loop and inner-loop, in order to perform switching between the brake and throttle controllers. The inner-loop controller containing the brake and throttle controllers is also called the servo control. Servo control tracks the reference value computed by outer loop controller, i.e. the reference value can be either the desired acceleration or the desired speed. In some cases the desired vehicle acceleration is applied to derive the required engine and brake torques. This is mainly because all engine management systems are torque-based which means that the air flow, ignition, fuel injection timing etc. are all set in the optimum position to deliver the required torque. In Shakouri, Ordys, Laila, and Askari (2011) and Riis (2007) the outer loop controller uses a conventional Proportional (P) control to derive a required speed, i.e. outer loop controller adapts the functionality of cruise control system through calculating the required vehicle speed to maintain the distance preset by the driver. The outer loop controller also contains switching function to implement switching between the driver's preset speed, i.e. cruise control speed, and the ACC control calculated reference speed.

Eventually, the inner loop controller regulates the brake pedal and throttle opening position to achieve the reference speed calculated by outer-loop controller in order to guarantee a flawless distance tracking from other vehicles as traffic speeds up and slows down. Following this approach, (Shakouri et al., 2011) has proposed various control methods including Gain Scheduling PI (GSPI) control, Gain Scheduling Linear Quadratic (GSLQ) control and Model Predictive Control (MPC) in design of inner loop controller (Fig. 1). Following this principle, inner loop controller is decoupled into the throttle controller and the brake controller by itself and their operation need to be coordinated by use of a proper switching logic.

A Model Predictive Controller (MPC) was employed by van den Bleek (2007) for designing an ACC system by using a linear model in which the states are distance between the following and the leading vehicles, the relative velocity and the following vehicle velocity and the states related to the dynamics of the vehicle were disregarded. Similar approach was followed by Jonsson (2003), there the desired acceleration is calculated by the outer-loop controller or master control loop. Furthermore, van den Bleek (2007) introduced two separate MPCs corresponding to throttle and brake controllers. Each MPC controller computes the desired acceleration for the throttle and the brake controllers. Subsequently, the calculated accelerations are converted to the throttle and the brake controlling signals through inner loop controller or slave control loop. Riis (2007) studied the optimisation of the fuel consumption through an ACC system for which the Nonlinear Model Predictive Controller (NMPC) was utilised.

A proper logical algorithm needs to be devised in order to provide smooth switching between the brake and the throttle controllers. The subject of coordinated switching between the brake and the throttle for the ACC application has been researched in the literature (Gerdes & Hedrick, 1997). Coordinated operation between the brake and throttle is crucial due to the following reasons:

- Frequent switching between the brake and the throttle or chattering has negative impact on the longitudinal dynamic of the vehicle as it causes the variation of vehicle's acceleration which provides an un-comfortable environment for passengers. Also, this behaviour causes rapid damage in vehicle's components.
- The frequent and rapid switching between throttle and brake causes loss of the energy, and therefore increases the fuel consumption.
- Inappropriate switching can be a source of instability and disturbance in the system which makes the control design task

more complicated. This effect is more crucial while using two control loops i.e. outer-loop and inner-loop controllers as the performance of each control loop affects the other one. Thus, any instability on the response of the outer-loop can be prompted by the performance of the inner-loop.

As it was explained previously, the common approach to the design of an ACC system is based on two loop controllers; inner-loop and outer-loop controllers. The inner-loop also comprises of two controllers; one controller is to regulate the throttle opening and the other one controls the brake position. From control design standpoint, the switching between two control systems, performing different tasks, is undesirable as it may cause instability and degrades the system performance. In this paper, a single control loop approach based on the nonlinear model predictive control (NMPC) has been utilised in developing an ACC system. A state-dependent algorithm, as an approach to control the brake and throttle opening position is proposed. Two Linear Time Invariant (LTI) discrete-time state space models, corresponding to modes of operation: accelerating – the throttle is active and braking – the brake is active, have been extracted from the full non-linear model of the vehicle and the power train. Those models are used to design the NMPC controller. From this prospective, a single but state-dependent MPC can be utilised in controlling the throttle and brake position which provides an easy approach to the control design process. Also, the objective of the distance tracking is incorporated into the single NMPC by extending the original LTI models. This is achieved by introducing the additional states corresponding to the relative distance between leading and following vehicles, and also the velocity of the leading vehicle. The proposed approach in this paper not only eliminates the need to design the additional control loop, i.e. outer-loop controller, to implement distance tracking control, but also improves the ACC performance by avoiding the chattering in the throttle opening and brake position control signals, which are the main contributions of the paper.

The controller designed in this work is implemented and tested in the MATLAB/SIMULINK® environment to control the nonlinear model developed in Shakouri et al. (2010). Some simulation results are provided, to show the performance of the proposed controller. Also the comparison with a representative more traditional structure in design of the ACC, namely the one presented in Shakouri et al. (2011) is carried out in which the throttle and brake are controlled by two separate controllers i.e. throttle is regulated by a linear Model Predictive Controller (MPC) and a PI controller is used to control the brake. Notice that this latter structure requires a sophisticated logical algorithm in order to proceed the switching between two controllers.

The paper is organised as follows. Section 2 presents the nonlinear dynamic model of the vehicle utilised for designing the controller, in addition, linearization of the nonlinear equations

of the vehicle, augmentation of the linear models with inter-vehicle dynamic are discussed in this section. Design of the ACC based on the method proposed in this paper, i.e. a single control loop by utilising NMPC, is carried out in Section 3, furthermore, the future reference trajectories corresponding to distance tracking and velocity tracking modes of the ACC are determined in this section. Performance of the ACC system is tested and the results presented in Section 4. Finally, conclusions of the paper are drawn in Section 5.

2. Vehicle model

Several dynamic models of the vehicle exist in the literature. Shakouri et al. (2010), Shakouri (2012), Majdoub, Giri, Ouadi, Dugard, and Chaoui (2012) investigates a group of models. Some of those models consider complex issues, such as the impact of the tyre on the vehicle performance, the load transfer between the front and rear axles during braking and acceleration etc. Some others are based on simplified equations. The comparison between the different models demonstrated that similar results could be obtained when the vehicle drives at high speed and there are no adverse road conditions, e.g. ice. The simple model is opted for, for the control design purpose in this paper.

The vehicle model used in this work is that of a passenger vehicle with automatic transmission system. The model is based on Shakouri et al. (2010) and Shakouri (2012). The vehicle dynamics is classified into two categories: (1) the dynamics of the power-train – consisting of the engine, the torque converter, the gear box, the final drive and the wheels; (2) the dynamics of the vehicle – considering the external forces acting on the vehicle and these include aerodynamic drag force, gravitational force and rolling resistance. The following equations are used to determine the dynamic model of the vehicle for the control design purpose.

The engine torque balance equation, considering the engine friction, the pumping losses and the load acting on the engine is given as

$$I_{ei}\dot{N}_e = \underbrace{T_{ei}(u_t, N_e) - T_f - T_p}_{T_{eb}} - \underbrace{\left(\frac{N_e}{K_{tc}}\right)^2}_{T_i} \quad (1)$$

Eq. (1) explains the mathematical relationship of the engine and impeller, with N_e the engine speed measured in rad/s, I_{ei} the summation of engine and impeller moment of inertia, T_{ei} the engine torque denotes the engine indicated torque (the torque before considering friction and pumping losses on the engine), T_f denotes the engine friction loss, T_p denotes the engine pumping loss and T_i denotes the impeller torque (acting load). The engine brake torque results from deducting the friction and pumping losses from the engine indicated torque and it is indicated by T_{eb} . The last term in (1) calculates the impeller (torque converter

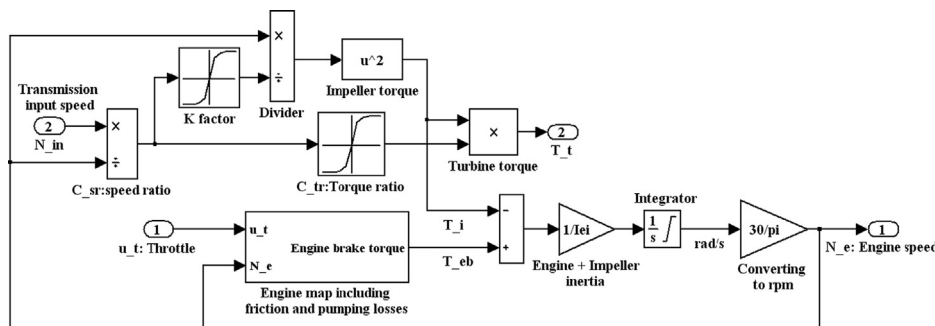


Fig. 2. The engine model considering friction and pumping losses, and the torque converter model.

Table 1

The value of the parameters used in simulation test.

Parameter	Description	Numerical value
m	Vehicle mass	1500.5 Kg
r	Wheel radius	0.326 m
R_{tr}	Gear ratio	[1:2.34; 2:1.45; 3:1.00; 4:0.68]
R_{fd}	Final driver ratio	3.28
I_{ei}	Moment of inertia of engine and torque converter	0.224 Kgm ²
τ_b	Lumped lag-servo valve and the hydraulic system	0.2 s
$\frac{1}{2}\rho A C_d$	Aerodynamic force coefficient	0.49 Kg/m
C_r	Rolling resistance coefficient	0.015
K_c	Pressure gain	1
K_b	Pressure/torque conversion constant	20 Nm/Bar
g	Gravitational acceleration	9.8 m/s ²

input) torque. K_{tc} is the capacity factor (K-factor). To present the model of the engine in the simulation, an engine map utilising the Jaguar Land Rover (JLR) data is applied which gives the engine brake torque vs. engine rotation speed rpm and the percentage of throttle opening position u_t . The engine simulation model is demonstrated in Fig. 2.

The parameters playing an important role in the performance of a torque converter are the speed ratio $C_{sr} = N_t/N_i$, the torque ratio $C_{tr} = T_t/T_i$, and the capacity factor (K-factor) $K_{tc} = N_e/\sqrt{T_i}$. Assuming solidity between the components, i.e. neglecting distortion and damping effect of rotating part, the impeller speed N_i and turbine (torque converter output) speed N_t can be considered to be the same as the engine speed N_e and transmission input speed N_{in} , respectively. Therefore, in this approach, the torque ratio C_{tr} and the capacity factor K_{tc} have been interpolated from the graph illustrating the performance characteristic of a torque converter vs. speed ratio C_{sr} from Wang (2001). The transmission input speed N_{in} is related to vehicle speed via following equation:

$$N_{in} = \frac{v_h R_f R_{tr}}{2\pi} \quad (2)$$

where, v_h denotes vehicle speed, R_{tr} is the gear ratio, R_f is the final drive ratio.

Thus, the speed ratio can be expressed as a function of the vehicle speed:

$$C_{sr} = \frac{v_h R_f R_{tr}}{2\pi N_e} \quad (3)$$

In the model of power train, the gear shifting is implemented through the gear shift logic based on the thresholds calculated by the respective blocks for up-shift and down-shift (Shakouri et al., 2010).

The torque generated in the wheel through the engine can be calculated by following equation:

$$T_{wheel} = R_{tr} R_f T_t = R_{tr} R_f C_{tr} \left(\frac{N_e}{K_{tc}} \right)^2 \quad (4)$$

where T_t is the turbine torque. Eq. (5) calculates the velocity of the vehicle by considering the torque produced on the wheel through the powertrain T_{wheel} , the braking torque T_b , aerodynamic force $F_{aerodynamic}$ and the last two terms in (5) defining the rolling resistance $F_{rolling-resistance}$ and the gravitational forces $F_{gravitational}$, respectively:

$$m\dot{v}_h = \frac{1}{r} \left[\underbrace{R_{tr} R_f C_{tr} \left(\frac{N_e}{K_{tc}} \right)^2}_{T_{wheel}} + T_b \right] - \underbrace{\frac{1}{2} \rho A C_d v_h^2}_{F_{aerodynamic}} - \underbrace{C_r m g \cos(\theta)}_{F_{rolling-resistance}} + \underbrace{m g \sin(\theta)}_{F_{gravitational}} \quad (5)$$

here ρ denotes the air density, C_d is the drag coefficient depending on the body shape, v_h velocity of vehicle and A is the maximum

vehicle cross area, m is the total mass of the vehicle, g is the gravitational acceleration, and θ varies depending on the road slope.

Finally, (6) calculates the braking torque as u_b is varied from 0 to -1 (Gerdes & Hedrick, 1997; Short, Pont, & Huang, 2004):

$$T_b = K_b P = K_b (150 K_c u_b - \tau_b \dot{P}) \leq 0 \quad (6)$$

where P is the amount of pressure produced behind the brake disk, τ_b is the lumped lag obtained by combining two lags relating to the dynamic of the servo valve and the hydraulic system, K_c is the pressure gain. K_b is a pressure/torque conversion for entire brake system. The values of the parameters are given in Table 1.

The vehicle dynamic model developed utilising (1)–(6) is non-linear whereas for the control design proposed here the model is required to be linearised. As a simplest approach, the nonlinear model is approximated in two operating points by two linear models through trimming procedure. These operating points are defined based on the modes of operation: accelerating-throttle is active, and braking-brake is active. Notice that changing between the accelerating and braking corresponds to, probably the most drastic change in the model structure. However, there are other non-linear effects, which could be taken into consideration, resulting in a larger number of linearised models. Those effects include: non-linear engine map and torque converter map, gear shifting and non-linear relationship between air resistance and velocity. These linear models are given as following state-space equations in continuous-time form:

$$\begin{aligned} \dot{x} &= A_{t(cont)} x + B_{t(cont)} u_t & (I) \\ \dot{x} &= A_{b(cont)} x + B_{b(cont)} u_b & (II) \end{aligned} \quad (7)$$

The state-space linear model (I) is valid when the throttle is active, while model (II) is obtained for operating of the brake. u_t and u_b are the throttle and brake controlled input, respectively. The subscript “cont” stands for continuous-time. The subscripts t and b denote that the state-space coefficients of each linear model ($A_{t(cont)}, B_{t(cont)}$) and ($A_{b(cont)}, B_{b(cont)}$) are correlated to the throttle and brake operating points, respectively. The numerical values of the coefficients are given in Appendix-A.

The states of the system are the brake pressure, the follower vehicle velocity and the engine angular speed (rpm) as $x = [P \ v_h \ N_e]^T$. The system output is the follower vehicle velocity v_h .

For development of the adaptive cruise control it's necessary to model the behaviour of the vehicle in front and then build a model of the overall system, including two vehicles (Fig. 4). In this paper the assumption is made that the vehicle in front travels at a constant speed, however, the variation of the leader vehicle velocity v_l acts as a disturbance on the system (Naus, Ploeg, van de Molengraft, Heemels, & Steinbuch, 2010). Hence:

$$\dot{v}_l = 0 \quad (8)$$

In practice, the distance between vehicles is measured by radar. However, in this paper for carrying out the simulation test, the distance between the rear end of the follower and leader vehicle can be determined by taking the integral of their relative velocity:

$$d(t) = \int_0^t (v_l - v_h) dt \quad (9)$$

Hence

$$\dot{d} = v_r = v_l - v_h \quad (10)$$

where v_l denotes the speed of the leading vehicle and it is assumed to be constant. d is the distance between vehicles. v_h is the velocity of the following vehicle.

In order to develop the state-space equation for the overall system, the states including the velocity of the leading vehicle and the distance between vehicles, i.e. $x_H = [v_l \ d]^T$, are added to the states of the vehicle's model:

$$x_{aug} = [P \ v_h \ N_e \ v_l \ d]^T \quad (11)$$

Thereby, the state-space models and their coefficients integrating the dynamic of the vehicle and the dynamic of the tracking (augmented dynamic) for the two modes of operation-throttle and brake- in the continuous-time are as follows:

$$\begin{aligned} \dot{x}_{aug} &= A_{t(aug)} x_{aug} + B_{t(aug)} u_t & (I) \\ \dot{x}_{aug} &= A_{b(aug)} x_{aug} + B_{b(aug)} u_b & (II) \end{aligned} \quad (12)$$

The numerical values used here are given in [Appendix-B](#). The subscript “aug” stands for augmented equation in continuous-time. The augmented system's output vector is $y_{aug} = [v_h \ d \ v_r]^T$.

3. Control structure

ACC operates in two different modes depending on the situation of the traffic ahead; Cruise Control (CC) mode, i.e. speed tracking mode-and ACC control mode, i.e. distance tracking mode. It operates in the CC mode when the road in front of the ACC equipped vehicle is clear, i.e. there is no vehicle within clearance distance. In this situation vehicle travels at the desired cruising speed which is set up by the driver. Once it has approached other vehicles (travelling at lower speed) it switches to distance tracking mode. In this mode ACC attempts to keep the vehicle within the desired distance headway ([Fig. 3](#)), by controlling the speed of the vehicle. The distance headway can be customised by the driver taking into account the braking time (time headway). The transition between the modes is performed automatically by considering the traffic condition ahead and the desired cruising speed.

In this paper, the ACC structure is developed based on a single control loop which implements the distance- and speed-tracking controls by using the Nonlinear Model Predictive Control (NMPC). The schematic block diagram of the ACC system is depicted in [Fig. 4](#). In order to conduct smooth and flawless distance- and speed- tracking, a single but state-dependent MPC is utilised in controlling the throttle and brake position. The switching between

throttle and brake is processed depending on the controller calculated output. Therefore, in order to control each of these components – the throttle and the brake – a switching algorithm is devised in such a way that the controlling signal sent to either throttle or brake is set to zero while the other one becomes active. The constraint on the control signal is imposed inside the controller to restrict it between $[-1,1]$. This comes from the physical limitation on the throttle and brake system. Furthermore, the controller output is implemented in the switching logic which works as below:

$$\begin{cases} u_t = u, \ u_b = 0 & 0 \leq u \leq 1 \\ u_b = u, \ u_t = 0 & -1 \leq u < 0 \end{cases} \quad (13)$$

u_t and u_b are the throttle and brake controlling signal respectively. u is calculated by the NMPC controller.

Inspecting the models for throttle and brake operation given by [\(12\)](#) leads to a conclusion that at the switching point (throttle equals zero and brake equals zero) the two models produce the same values of the output. At the switching point, e.g. $u=0$, the difference in the two models is in the structure of the matrices A . It can be noticed that both matrices are finite, hence, for any state x , when switching between the matrices, the derivative: \dot{x}_{aug} is finite. Hence, the function $x(t)$ is continuous at the switching point. Note: the derivative of the function may not be continuous (jump in the value of \dot{x}_{aug} is possible), but the outputs of the system are related to states, not state derivatives.

The desired distance headway, d_{des} can be computed using the following equation assuming that the follower and leader vehicles have the same speed $v_h=v_l$, which is known as constant-time headway policy ([Zhou & Zhang, 2003; van den Bleek, 2007](#)):

$$d_{des} = l + d_s + T_h v_h \quad (14)$$

where l is the vehicle length, d_s is the additional distance between two vehicles in order to avoid collision, v_h is host vehicle's velocity and T_h is constant-time headway can be approximated by the human reaction time i.e. 1.5–2 s ([Martinez & Canudas-de-Wit, 2007](#)).

3.1. Nonlinear Model Predictive Control (NMPC)

In this paper, two linear models are used and the choice of the model depends on the input signal. The approach proposed here to solve NMPC problem is based on methods used in [Dutka, Ordys, and Grimble \(2005\)](#), [Youssef, Ordys, and Grimble \(2004\)](#) and [Kouvarikakis, Canon, and Rossiter \(1999\)](#) where the nonlinear system is approximated by several linear models at various operating points. Hence, the parameters of the linear models are the functions of the state of the system. To adopt this approach in design of the ACC system, in lieu of the models being functions of the states, they are related to the controlled input. The state-space model may vary depending on the value of the controlled inputs predicted over future horizon. The negative value of the controlled input at a certain step in the future ascertains the need to apply the brake and results in utilising its associated state-space model in calculation of optimal control problem. The positive value

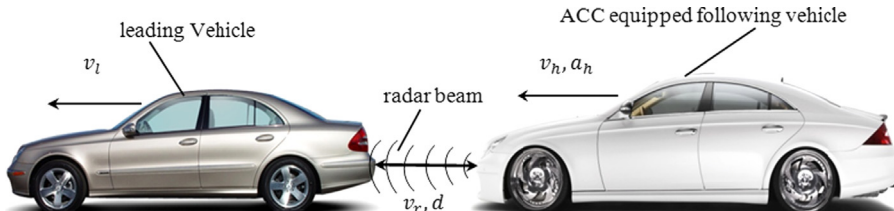


Fig. 3. An ACC equipped vehicle following another vehicle in front.

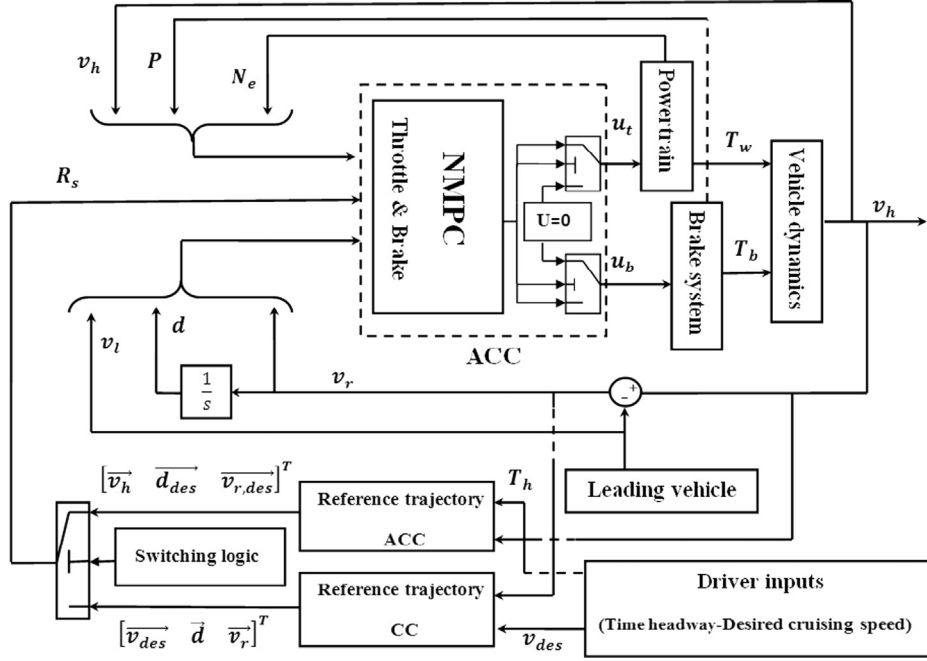


Fig. 4. Schematic block diagram of ACC algorithm including a single NMPC for controlling throttle and brake and a switching logic in order to implement transition between ACC and CC.

identifies that the throttle needs to be used, together with its associated model.

3.2. Developing NMPC equations for ACC problem

The model of the overall system (12) is discretised with the assumption of the sampling time, resulting from the sampling of on-board car control system. In this article this is assumed to be 0.1 s.

Thereby, the state-space equations and their coefficients integrating the dynamics of the vehicle and the dynamics of the tracking in association with brake and throttle operating modes are given as following equations in discrete-time:

$$x_{\text{aug}}(t+1) = \begin{cases} A_{t(\text{augd})}x_{\text{aug}}(t) + B_{t(\text{augd})}u(t), & u \geq 0 \\ A_{b(\text{augd})}x_{\text{aug}}(t) + B_{b(\text{augd})}u(t), & u < 0 \end{cases} \quad (15)$$

The subscript “augd” stands for augmented equation in discrete-time. The numerical values used here are given in Appendix-C.

In ACC system, NPMC computes the optimal controlled input such that the output parameters of the system, i.e. $y_{\text{aug}} = [v_h \ d \ v_r]^T$, reach the desired set-point determined by the vector R_s . To find the optimal solution for the system with one input and three outputs in MPC context, the output vector y can be decoupled into three separate outputs, y_1 , y_2 and y_3 as below:

$$y_{\text{aug}} = \begin{bmatrix} y_1 \\ y_2 \\ y_3 \end{bmatrix} = \begin{bmatrix} 0 & 1 & 0 & 0 & 0 \\ 0 & 0 & 0 & 0 & 1 \\ 0 & -1 & 0 & 1 & 0 \end{bmatrix} x_{\text{aug}} = \begin{bmatrix} C_{1(\text{augd})} \\ C_{2(\text{augd})} \\ C_{3(\text{augd})} \end{bmatrix} x_{\text{aug}} \quad (16)$$

The state-space equations of the system can be extended by taking the integral action into consideration (Liuping, 2009). This way, a differential state-space model is obtained for each of the output above.

$$\begin{aligned} \tilde{x}_i(t+1) &= A_{j,i}(t)\tilde{x}_i(t) + B_{j,i}(t)\Delta u(t) \\ y_i(t) &= C(t)\tilde{x}_i(t) \end{aligned} \quad (17)$$

$$\tilde{x}_i(t) = \begin{bmatrix} \Delta x_{\text{aug}}(t) \\ y_i(t) \end{bmatrix} \quad (18)$$

where $\Delta x_{\text{aug}}(t)$ and $\Delta u(t)$ are respectively the differences of the states and control variable and are given as: $\Delta x_{\text{aug}}(t) = x_{\text{aug}}(t) - x_{\text{aug}}(t-1)$, and $\Delta u(t) = u(t) - u(t-1)$. The subscript $i=1, 2, 3$ indicates the sequence of elements in output vector (16). The subscript $j=t$, b denotes the augmented model corresponding to operation modes i.e. brake and throttle. Therefore, six incremental matrices need to be calculated with respect to two subjects: mode of the operation and the sequence of the elements in the output vector. The numerical values for the six state-space representations are in Appendix-D.

To calculate the optimal controlled input within MPC context based on three independent outputs, the following performance index is required to be minimised:

$$J = (R_{s1} - Y_1)^T(R_{s1} - Y_1) + (R_{s2} - Y_2)^T(R_{s2} - Y_2) + (R_{s3} - Y_3)^T(R_{s3} - Y_3) + \Delta U^T \bar{R} \Delta U \quad (19)$$

where vectors $Y_{(1)}$, $Y_{(2)}$ and $Y_{(3)}$ are the predicted outputs of the system within prediction horizon N . $R_{s(1)}$, $R_{s(2)}$ and $R_{s(3)}$ are the set-point vectors associated with each output vector. \bar{R} is a weighing matrix, i.e. $\bar{R} = r_w I_{N \times N}$, where r_w positive. ΔU is the optimal control vector within control horizon N . $Y_{(1)}$, $Y_{(2)}$ and $Y_{(3)}$ can be determined by the following formulae:

$$Y_i = F_i \tilde{x}_i + \phi_i \Delta U \quad (20)$$

$\tilde{x}_{(i)}$ is initial state of the system at time instance t . Subscript i indicates the number of the associated output, i.e. $i=1, 2, 3$. The non-linear character of the system is captured in the formulation of matrices F_i and ϕ_i which contain parameters of “brake models” and “throttle models” (15) simultaneously. For details, the Reader is referred to Dutka et al. (2005). Matrices F_i and ϕ_i are defined as follows:

$$F_i(t, N) = \begin{bmatrix} C(t)[\prod_{n=1}^1 A_{j,i}(t+n)] \\ C(t)[\prod_{n=1}^2 A_{j,i}(t+n)] \\ C(t)[\prod_{n=1}^3 A_{j,i}(t+n)] \\ \vdots \\ C(t)[\prod_{n=1}^N A_{j,i}(t+n)] \end{bmatrix} \quad (21)$$

$$\varnothing_i(t, N) = \begin{bmatrix} C(t)[\prod_{n=1}^0 A_{j,i}(t+n)] B_{j,i}(t) & 0 \\ C(t)[\prod_{n=1}^1 A_{j,i}(t+n)] B_{j,i}(t) & C(t)[\prod_{n=2}^1 A_{j,i}(t+n)] B_{j,i}(t+1) \\ \vdots & \vdots \\ C(t)[\prod_{n=1}^{N-1} A_{j,i}(t+n)] B_{j,i}(t) & C(t)[\prod_{n=2}^{N-1} A_{j,i}(t+n)] B_{j,i}(t+1) \\ \dots & C(t)[\prod_{n=N}^{N-1} A_{j,i}(t+n)] B_{j,i}(t+N_c-1) \end{bmatrix} \quad (22)$$

where;

$$[\prod_{n=l}^t A_{j,i}(n)] = \begin{cases} A_{j,i}(t)A_{j,i}(t-1)\dots A_{j,i}(l) & \text{if } l \leq t \\ I & \text{if } l > t \end{cases} \quad (23)$$

Firstly, assume that the vector of the future controls, i.e. $\Delta U_N(t) = [\Delta u(t+1), \Delta u(t+2), \Delta u(t+3)\dots \Delta u(t+N)]$, is known. Note that such vector is calculated as a part of MPC procedure. Having $\Delta U_N(t)$ calculated within the control horizon N , the vector containing the absolute values of the control signals can be calculated as following vector:

$$U_N(t) = \left[\underbrace{u(t)+\Delta u(t+1)}_{u(t+1)}, \underbrace{u(t+1)+\Delta u(t+2)}_{u(t+2)}, \dots, \underbrace{u(t+N-1)+\Delta u(t+N)}_{u(t+N)} \right] \quad (24)$$

From vector calculated by (24), the incremental matrices $A(t)$ and $B(t)$ can be selected for the time instances. Switching between the models approximated based on modes of operation-brake and throttle, is implemented within the prediction horizon ($n=1, 2\dots N$), i.e. when the control sig:

$$\begin{cases} A_{t,i}(t+n), B_{t,i}(t+n) & 0 \leq u(t+n) \leq 1 \\ A_{b,i}(t+n), B_{b,i}(t+n) & -1 \leq u(t+n) < 0 \end{cases} \quad (25)$$

The incremental equations given by (17) and (18) must be calculated with regard to two subjects; mode of operation and type of output. Therefore, six incremental equations should be found in order to design the NMPC using state-dependent representation of the system, as explained in Table 2. As, three outputs have been considered in the design, three pair of $F_{i=1,2,3}$ and $\varnothing_{i=1,2,3}$ should be calculated subsequently for which matrices $A_{i=1,2,3}(t)$ and $B_{i=1,2,3}(t)$ vary within prediction horizon according to the logic defined by (25).

Assuming for a moment that the input signals are not constrained, the solution to the optimisation problem defined by (19), with equality constraints (17) and (20) is given by (Liuping, 2009):

$$\Delta U = \left(\sum_{i=1}^q [\varnothing_i^T \varnothing_i] + \bar{R} \right)^{-1} \left(\sum_{i=1}^q [\varnothing_i^T (R_{si} - F \tilde{x}_i(t))] \right) \quad (26)$$

where q is the number of the output and it equals 3 for our system. Thereby, $F_{i=1,2,3}$ and $\varnothing_{i=1,2,3}$ must be calculated utilising the incremental matrices (17) and (18) which need to be obtained for each output, separately, i.e. y_1, y_2 and y_3 . y_1, y_2 and y_3 are associated with v_h, d and v_r , respectively. The set-point vectors R_{s1}, R_{s2} and R_{s3} corresponding to each output must be defined.

The solution given by Eq. (26) may be feasible in many practical situations, because it is rare that while driving a vehicle in a reasonable way the driver would wish to apply more than 100% of

throttle opening or more than 100% braking force. Hence, it may be advisable to programme the control algorithm in such a way that this unconstrained solution is calculated first and the programme checks whether it is feasible. However, in general, the feasibility cannot be guaranteed, as the optimisation is performed over a certain horizon into the future. Hence, the constrained version is also calculated.

3.2.1. Constraints on the controlled input

In the vehicle model, the throttle opening position u_t varies from 0 to 1 and subsequently the brake pedal position u_b is restricted between 0 and -1 . Therefore, the constraints need to be imposed on the controlled input calculated by NMPC as $-1 \leq u \leq 1$. In order to incorporate the constraints in the implementation of Model Predictive Control (MPC) the Hildreth's Quadratic Programming is utilised (Liuping, 2009). In our control design, the optimisation problem is solved by taking into account the constraint on the amplitude of the control variable as given below:

$$\underbrace{\begin{bmatrix} 1 & 0 & \dots & 0 \\ 1 & 1 & \dots & 0 \\ 1 & 1 & \ddots & 0 \\ 1 & 1 & \dots & 1 \\ -1 & 0 & \dots & 0 \\ -1 & -1 & \dots & 0 \\ -1 & -1 & \ddots & 0 \\ -1 & -1 & \dots & -1 \end{bmatrix}}_{A_{\text{cons}}} \underbrace{\begin{bmatrix} \Delta u(t+1) \\ \Delta u(t+2) \\ \vdots \\ \Delta u(t+N_c) \end{bmatrix}}_{\Delta U} \leq \underbrace{\begin{bmatrix} u_{\max} - u(t) \\ u_{\max} - u(t) \\ \vdots \\ u_{\max} - u(t) \\ u_{\min} + u(t) \\ u_{\min} + u(t) \\ \vdots \\ u_{\min} + u(t) \end{bmatrix}}_{\gamma} \quad (27)$$

The dimension of matrix A_{cons} is $N_c \times 2N_c$, and the dimension of both vectors ΔU and γ are $1 \times N_c$. u_{\max} and u_{\min} are the upper and lower bound of the constraint, respectively, i.e. $u_{\max} = 1$ and $u_{\min} = -1$. The solution to the Hildreth's programming is based on Karush–Kuhn–Tucker multipliers.

A standard iterative procedure is used to solve this problem, which is affine with respect to the equality constraints (the state-space models) and quadratic with respect to the objective functions (performance index). Hence, the conditions of regularity for Karush–Kuhn–Tucker optimisation problem are met for all linearised models, (see e.g. Ruszczyński, 2006).

The feasibility of the solution is defined as availability (existence) of a solution for each operating condition. Notice that the model is a linear state-space equation and the constraints are applied only on the inputs to this equation. Furthermore, the constraints, as defined by inequality (27) are affine. It is easy to see that, for $u_{\max} = 1$ and $u_{\min} = -1$ there always exists a solution to this inequality. Hence, the feasibility is guaranteed. For every possible state of the system, the next state exists, because the set of available inputs is non-empty.

The schematic block diagram of NMPC illustrating the steps for calculation of the controlled input is depicted in Fig. 5.

3.2.2. Future set-point trajectory

The reference set-point R_s is required for calculation of control sequence whithin MPC contex. The reference trajectory is different

Table 2

The incremental matrices $A_{i=1,2,3}$, $B_{i=1,2,3}$ and C and matrices $F_{i=1,2,3}$ and $\varnothing_{i=1,2,3}$ are classified according to modes of operation and corresponding outputs.

Operation	Output					
	$y_1=v_h$		$y_2=d$		$y_3=v_r$	
Throttle	F_1	$A_{t,1}, B_{t,1}, C$	F_2	$A_{t,2}, B_{t,2}, C$	F_3	$A_{t,3}, B_{t,3}, C$
Brake	\varnothing_1	$A_{b,1}, B_{b,1}, C$	\varnothing_2	$A_{b,2}, B_{b,2}, C$	\varnothing_3	$A_{b,3}, B_{b,3}, C$

depending upon whether the system operates in ACC mode or CC mode. Considering the output equation of the system given by (12), three outputs are the vehicle velocity v_h , the distance d and the relative speed v_r . When the system is in the CC mode, the only parameter being of concern is the vehicle speed, while the relative speed and the distance do not need to follow a reference trajectory i.e. are “free”. However, when the system operates in the ACC mode, the relative velocity and the distance are important parameter while vehicle speed is “free”. To perform optimisation numerically, we want to make sure that the performance index (19) is not optimised with respect to those variables which do not need to follow a reference. The way of achieving that is by setting the appropriate reference signal equal to the predicted future values of those “free” variables.

So far, we explained the method used to select the variables to be included in the vector of reference signals, depending on the mode of the operation (CC or ACC). Next, we explain how the future values of reference signals are generated for each mode. For CC mode the future reference trajectories are the predicted desired cruising speed \vec{v}_{des} , the predicted distance \vec{d} and the predicted relative velocity \vec{v}_r . While the predicted vehicle speed \vec{v}_h , the predicted desired distance \vec{d}_{des} and the predicted desired relative velocity $\vec{v}_{r,des}$ are the future reference trajectory introduced for the ACC mode.

When the system detects the preceding vehicle, it tries to follow it at a desired distance, i.e. the system operates in the ACC mode. The desired distance is calculated based on the constant

time-headway policy (14). To extend (14), to cover the future prediction horizon, the velocity of the following vehicle needs to be predicted first. It can be achieved by estimating the state of the system over the prediction horizon. Notice that the augmented state of the system (11) contains both of distance and velocity as both states and outputs. Hence using the same output prediction equation as in (20) and employing the augmented matrices $A_{t(augd)}$, $A_{b(augd)}$, $B_{t(augd)}$, $B_{b(augd)}$, $C_{1(augd)}$, the future values of those can be calculated. Therefore, Matrices F_i and ϕ_i given by (21)–(23) must be calculated using the augmented Eq. (19) in association with both modes of operation, i.e. throttle and brake. Next, the system output, i.e. prediction of the vehicle's velocity, will be calculated utilising (20) by having the initial state of the system $x_{augd} = [P \ v_h \ N_e \ v_l \ d]^T$ and the absolute value of the optimal control vector U given by (24):

$$\vec{v}_h = Fx_{augd} + \phi U \quad (28)$$

Table 3
Logical rule for switching between CC and ACC.

$v_h < v_{des}$	$v_h \geq v_{des}$ and $v_r < 0$	$v_h \geq v_{des}$ and $v_r \geq 0$
$d \leq d_{des}$	ACC	ACC
$d > d_{des}$	CC	CC

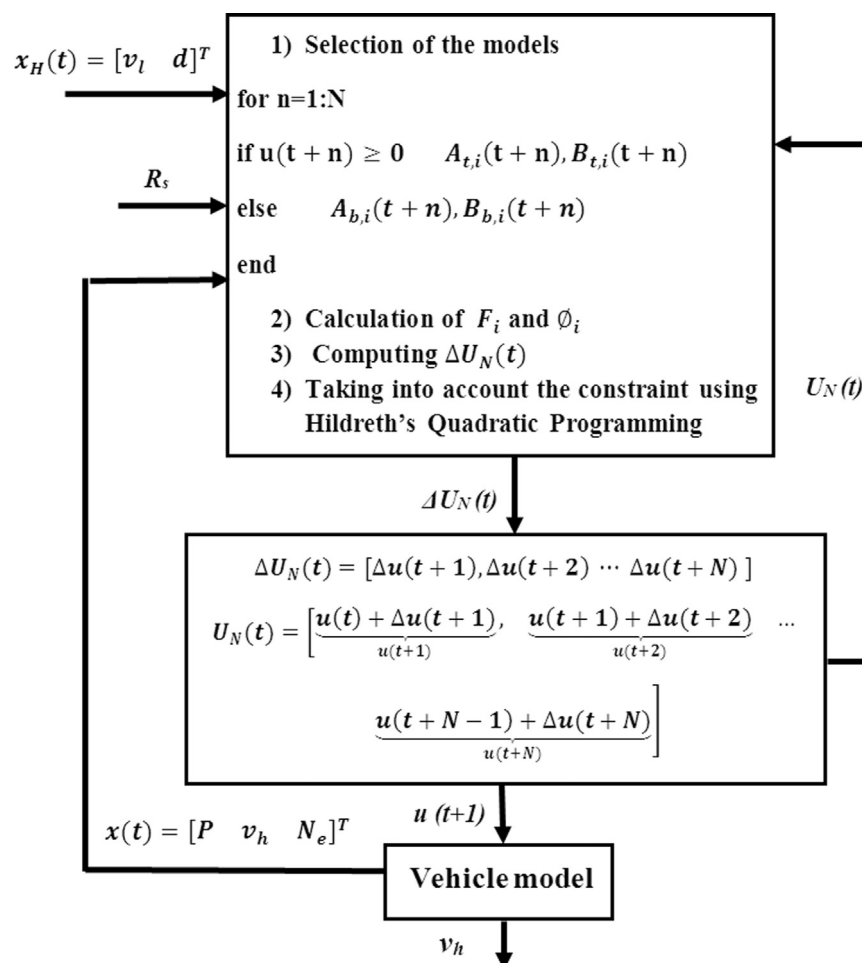


Fig. 5. Schematic diagram of NMPC structure illustrating the steps for calculation of the controlled input sequence $U_N(t)$ over the future horizon at each instance of time t –the first element of the sequence $u(t+1)$ is sent to the vehicle model.

Having the predictive velocity of the vehicle within future horizon v_h , the trajectory of desired distance between the vehicles can be predicted by the following equation:

$$\overrightarrow{d}_{des} = l + d_s + T_h \overrightarrow{v}_h \quad (29)$$

Additional reference trajectory needs to be introduced when the system operates in the ACC mode is the relative velocity, i.e. the difference of the velocity of the following and leading vehicle. The relative velocity should be zero during operating the system in the ACC mode:

$$\overrightarrow{v}_{r,des} = O_{N \times 1} \quad (30)$$

$\overrightarrow{v}_{r,des}$ is desired relative distance over prediction horizon.

If there is no vehicle detected in front of the vehicle equipped with ACC, the system switches over CC and it attempts to follow the speed set up by driver, i.e. desired cruising speed. The reference trajectory in this case would be constant within the future horizon:

$$\overrightarrow{v}_{des} = I_{N \times 1} v_{des} \quad (31)$$

\overrightarrow{v}_{des} is a vector defining the desired velocity over future prediction horizon. v_{des} is the scalar value. $I_{N \times 1}$ is the vector which its elements are one. Subscript N is prediction horizon.

For simplicity, \overrightarrow{v}_r and \overrightarrow{d} can be assumed to be constant over future horizon:

$$\overrightarrow{v}_r = I_{N \times 1} v_r \quad (32)$$

$$\overrightarrow{d} = I_{N \times 1} d \quad (33)$$

v_r and d are the scalar values correlating to the relative velocity and the real distance between vehicles, respectively. \overrightarrow{v}_r and \overrightarrow{d} are predicted values of those parameters over the future horizon. $I_{N \times 1}$ is the vector which all its elements are one. Subscript N is prediction horizon. In a more precise way, the method has been

explained previously for prediction of the vehicle's velocity given by (28) can be utilised to calculate \overrightarrow{v}_r and \overrightarrow{d} . It can be done by using the vehicle models corresponding to the distance and the relative velocity which their state-space coefficients are $[A_{t(augd)}, A_{b(augd)}, B_{t(augd)}, B_{b(augd)}, C_{2(augd)}]$ and $[A_{t(augd)}, A_{b(augd)}, B_{t(augd)}, B_{b(augd)}, C_{3(augd)}]$ respectively.

In order for the ACC system to be able of switching between the ACC and CC modes, the synthesised switching logic need to be devised to precisely perform transition from ACC to CC and vice versa. The switching logic functions such a way that the calculated reference trajectories corresponding to both ACC&CC modes pass through the gate so as to be exploited by NMPC for calculation of the optimal control sequence. The logical condition of the switching is illustrated in Table 3. If the actual distance is less than the desired distance, the system switches to the distance control mode (ACC mode), otherwise the vehicle operates in the CC mode. Further condition for implementing the switching between the modes is the speed. In the ACC mode, if the leading vehicle increases its speed, the following vehicle keeps tracking it, i.e. remains in ACC mode, until its speed reaches the desired cruising speed. At this moment, the system reverts to CC mode. Furthermore, to consider the potential safety hazard and to avoid rear end collision, the relative velocity is included in the switching algorithm.

3.3. Tuning parameters

This paper intends to overcome the shortcomings of previous approaches to brake/throttle control for ACC/CC. Those shortcomings include the jerk (acceleration variation) and instability due to frequent switching between brake and throttle manipulation. It will be shown in Section 4 that the controller action can be made smooth through the tuning of MPC, i.e. selection of various parameters in the MPC cost function. In the proposed design, although two models are used to describe the powering and braking processes and those are controlled by two independent

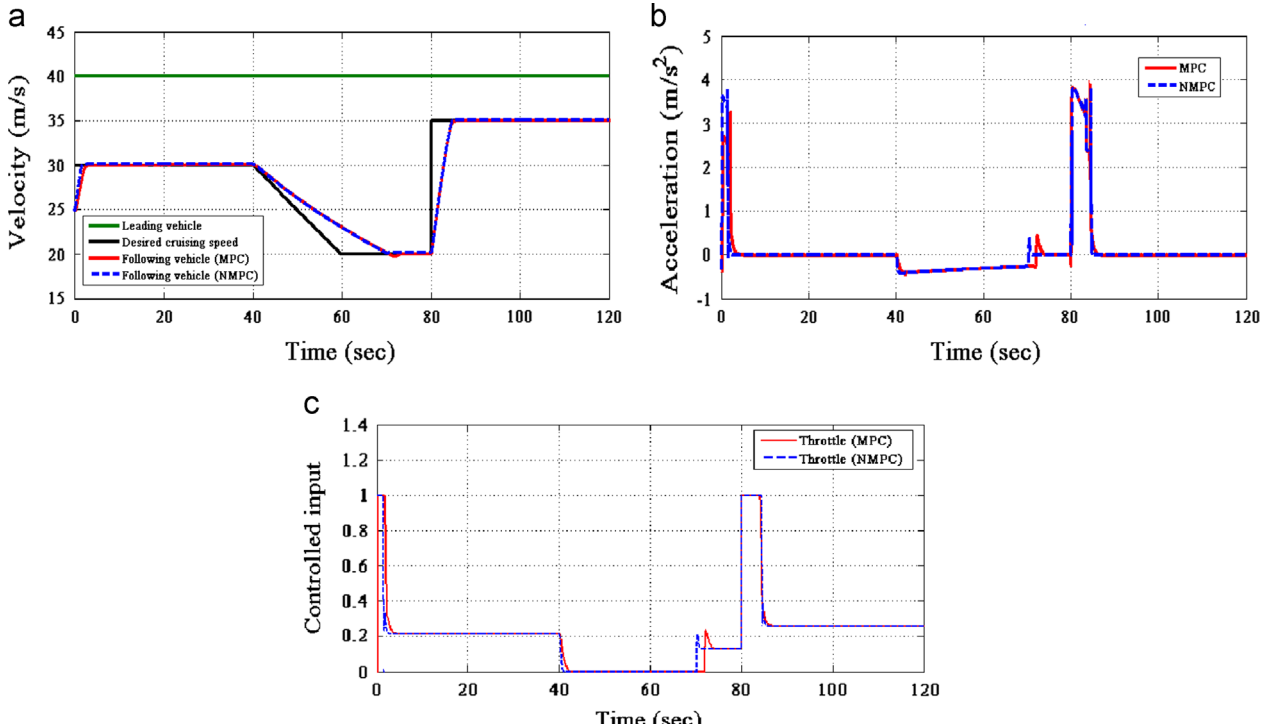


Fig. 6. The ACC system operates in CC mode, (a) velocities: leading vehicle, following vehicle: desired cruising speed, the actual speed when using MPC and the actual speed when using NMPC, (b) the acceleration of the vehicle – the results of two controllers are compared, and (c) comparison of throttle signals for NMPC and MPC cases.

control inputs (throttle and brake), from the control design perspective there is one input (positive or negative, constrained between -1 and 1), which affects the torque upon the driveline. Sudden change of torque introduces intensive jerk. However, MPC performance index contains the vector: ΔU which represents the derivative (speed of change) of the control input. By selecting the weight associated with ΔU (r_w) it is possible to adjust the smoothness of the control signal, hence the jerk. Also, the switching between braking and accelerating would be reduced/eliminated if ΔU is penalised. This is illustrated by simulation results in the next section. The simulation results were initially obtained (Figs. 6 and 7) by setting up the values of tuning parameters r_w and N as 25 and 30 , respectively. However, as explained in Section 4, then the value of r_w in the NMPC algorithm has been increased to 180 to remove chartering from the results. The larger prediction horizon N would increase the computational time, due to increasing the dimensions of the prediction matrices. The tuning parameters have been chosen based on the trade-off between the computational time and the performance of the control algorithm. The computational time measured for the selected sampling time in this article (i.e. 0.1 s) is approximately 0.009 s, which makes the proposed algorithm feasible for the real-time application.

4. Simulation and results

The system proposed in this paper has been tested, using the nonlinear model and the control design obtained earlier with the parameters provided in Appendix, in different traffic scenarios:

Velocity tracking (CC) mode: The system operates in this mode when the distance between vehicles is greater than the desired distance. Also, the system can enter this mode, if the leading vehicle speed becomes higher than the desired cruising speed.

Distance tracking (ACC) mode: The system operates in the ACC mode, when the vehicle approaches the vehicle travelling (slower) in front of it. Then, the distance between vehicles is maintained.

Switching mode: The system may switch between the modes-CC and ACC- depending on the condition on the road.

Stop & go mode: This situation occurs when the vehicle has to frequently stop and move, depending on the behaviour of other vehicles in the traffic. When the traffic slows down and comes to standstill, the vehicle equipped with ACC needs to slow down and stop for a while, until the vehicle in front starts moving.

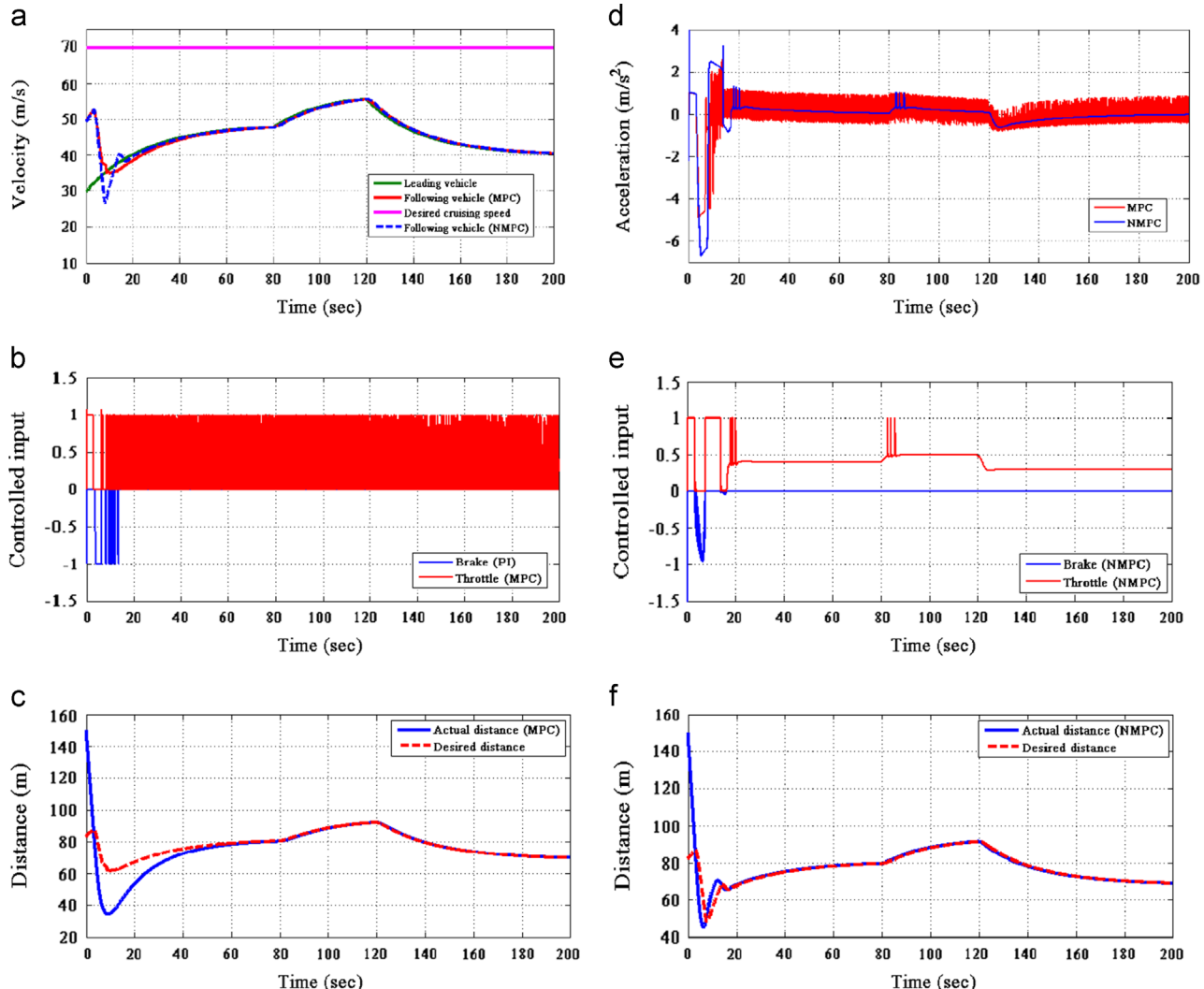


Fig. 7. The system operates in ACC mode – first set of results, (a) velocity: leading vehicle, following vehicle: desired cruising speed, the actual speed when using MPC and the actual speed when using NMPC, (b) throttle and brake signals for MPC case-brake is controlled by PI controller, while throttle by MPC, (c) distance between vehicles when using MPC algorithm, (d) the acceleration of the vehicle – the results of two controllers are compared, (e) throttle and brake signals – both brake and throttle are controlled by a single NMPC, and (f) distance between vehicles when using NMPC algorithm.

A common approach in designing the ACC is based on two separate control loops; Outer-Loop Controller (OLC) and Inner-Loop Controller (ILC) (Shakouri et al., 2011). In this paper, this common approach serves as a reference point – to compare with the algorithm proposed in this paper. The schematic block diagram of an ACC system based on this structure is depicted in Fig. 1. The outer-loop controller calculates the reference velocity using a PI (proportional-integral) controller attempting to maintain the desired distance between vehicles. The inner-loop controller regulates the throttle and brake in order to track the calculated reference velocity. Inner-loop controller consists of two separate controllers to regulate the brake and the throttle. Here, a Linear Model Predictive Control (MPC) is utilised to control the throttle opening, while a PI controller is employed for controlling the brake. The MPC is designed by using only one linear state-space model approximated for throttle operation (brake is inactive). PI controller is tuned by using the linear model obtained for brake operation (throttle is inactive). These linear models are the same as the one used for designing the NMPC. The performance of the approach proposed in this paper, i.e. utilising a single control loop, is compared with the ACC algorithm built up from two control loops.

The results of comparison demonstrate that the method proposed in this paper can improve the performance of the ACC system by

avoiding chattering on throttle opening and brake actions which may result from switching between throttle and brake controllers. Furthermore, any disturbance caused by the outer loop controller can provoke the chattering in the control actions. Although, the chattering may not affect the tracking performance of the ACC system, it causes the high frequency acceleration which downgrades the driving comfort. For abridgment purpose in the considerations below, the ACC structure employing two separate controller's loops is denoted as MPC.

Fig. 6 shows the results of the simulation when the system operates in CC mode. The desired cruising speed is less than the leading vehicle's velocity. The initial speed of the following vehicle is 25 m/s, and the initial distance between leading and following vehicle is higher than the desired distance. The desired cruising speed is defined in the form illustrated in Fig. 6a. Since, there is no risk posed by the surrounding traffic conditions in the CC mode, and also for the purpose of fuel efficiency and driving comfort, it is not necessary to apply the brake. Therefore, the throttle is only manipulated to control the vehicle velocity. Fig. 6c illustrates the variation of the throttle signals in order for the vehicle's velocity follows the desired cruising speed which is set lower than the leading vehicle's velocity. The acceleration of the vehicle during CC mode is depicted in Fig. 6b. The results of comparison between two control applications, i.e. MPC &

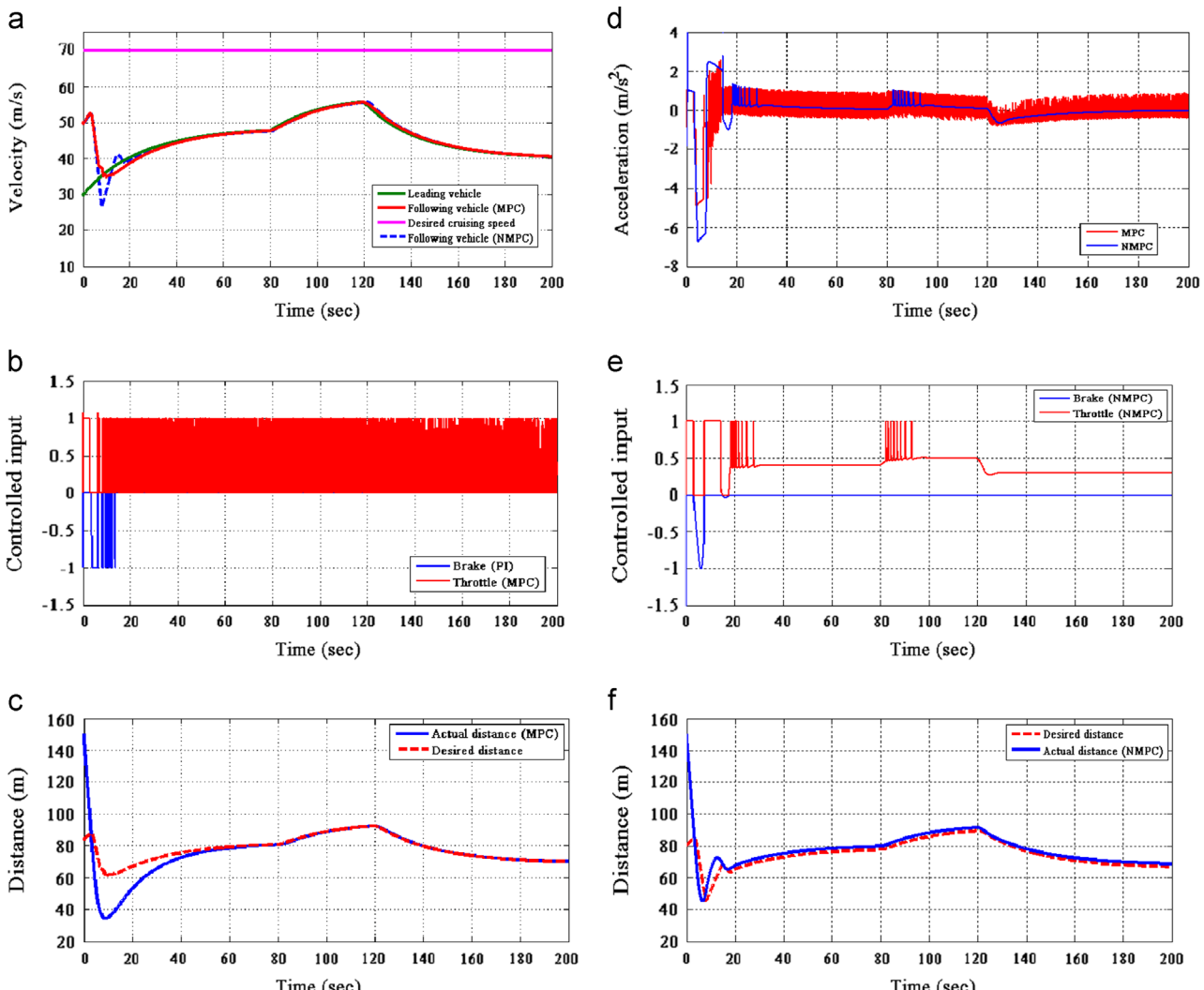


Fig. 8. The system operates in ACC mode – second set of results – r_w has been increased, (a) velocity: leading vehicle, following vehicle: desired cruising speed, the actual speed when using MPC and the actual speed when using NMPC, (b) throttle and brake signals for MPC case-brake is controlled by PI controller, while throttle by MPC, (c) distance between vehicles when using MPC algorithm, (d) the acceleration of the vehicle – the results of two controllers are compared, (e) throttle and brake signals – both brake and throttle are controlled by a single NMPC, and (f) distance between vehicles when using NMPC algorithm.

NMPC, show the similar performance of system in velocity tracking mode. However, the MPC demonstrates a small undershoot at tracking the lower set-point speed (20 m/s) (Fig. 6a). Furthermore, the NMPC is slightly faster at increasing speed between 25 and 30 m/s, which results in larger acceleration (Fig. 6b).

Fig. 7 shows the simulation results for ACC mode. In order to implement this particular test, desired cruising speed is set up at a value higher than the leading vehicle's velocity. The vehicle equipped with ACC system is running with initial speed of 50 m/s and it is at distance 150 m from leading vehicle. Initially, the distance is greater than the desired distance and the vehicle's velocity increases for almost 5 s. As the vehicle equipped with ACC approaches the leading vehicle (Fig. 7b), it applies the brake (Fig. 7c) to follow the leading vehicle within the desired distance. The comparison between two approaches (MPC and NMPC) demonstrates that the proposed method, based on the NMPC, provides considerably better functionality of the ACC system in the distance tracking mode, in terms of good tracking the desired distance and in terms of smoothing out chattering in the acceleration curve. Fig. 7f shows that the ACC employing NMPC reacts faster when the following vehicle, travelling at a higher speed, approaches the leading vehicle, so that the velocity is reduced quickly and the desired distance to the leading vehicle is

maintained better. In the approach using MPC the vehicle is allowed to get closer to the leading vehicle. Furthermore, utilising a single NMPC provides a more uniform acceleration and deceleration compared to the control structure which uses MPC for regulating throttle opening and a PI controller to control the brake pedal position (Fig. 7d). Uncomfortable variation of the vehicle acceleration is a consequence of the chattering in throttle opening and brake position (Fig. 7b). However, in this case, chattering still exists in the controlled inputs when using NMPC.

Despite good performance of the NMPC, still some chattering in the controlled inputs (throttle opening and brake) can be observed at some parts of the response as illustrated in Fig. 7e. Some of the chattering (chattering in brake action) can be removed by increasing the tuning parameter r_w . The results are presented in Fig. 8. Fig. 8e shows that, when increasing the tuning parameter, chattering is removed in the brake input of NMPC, but some still remains in throttle opening input. There is also a minimal deterioration of the performance with respect to tracking the desired distance.

Further removal of the chattering can be obtained by introducing a dead-zone for the distance error in the controller implementation. The results of those tests are presented in Fig. 9. Notice that in case of MPC, introducing the dead zone would not remove the chattering. This is because, the chattering in MPC is due to two

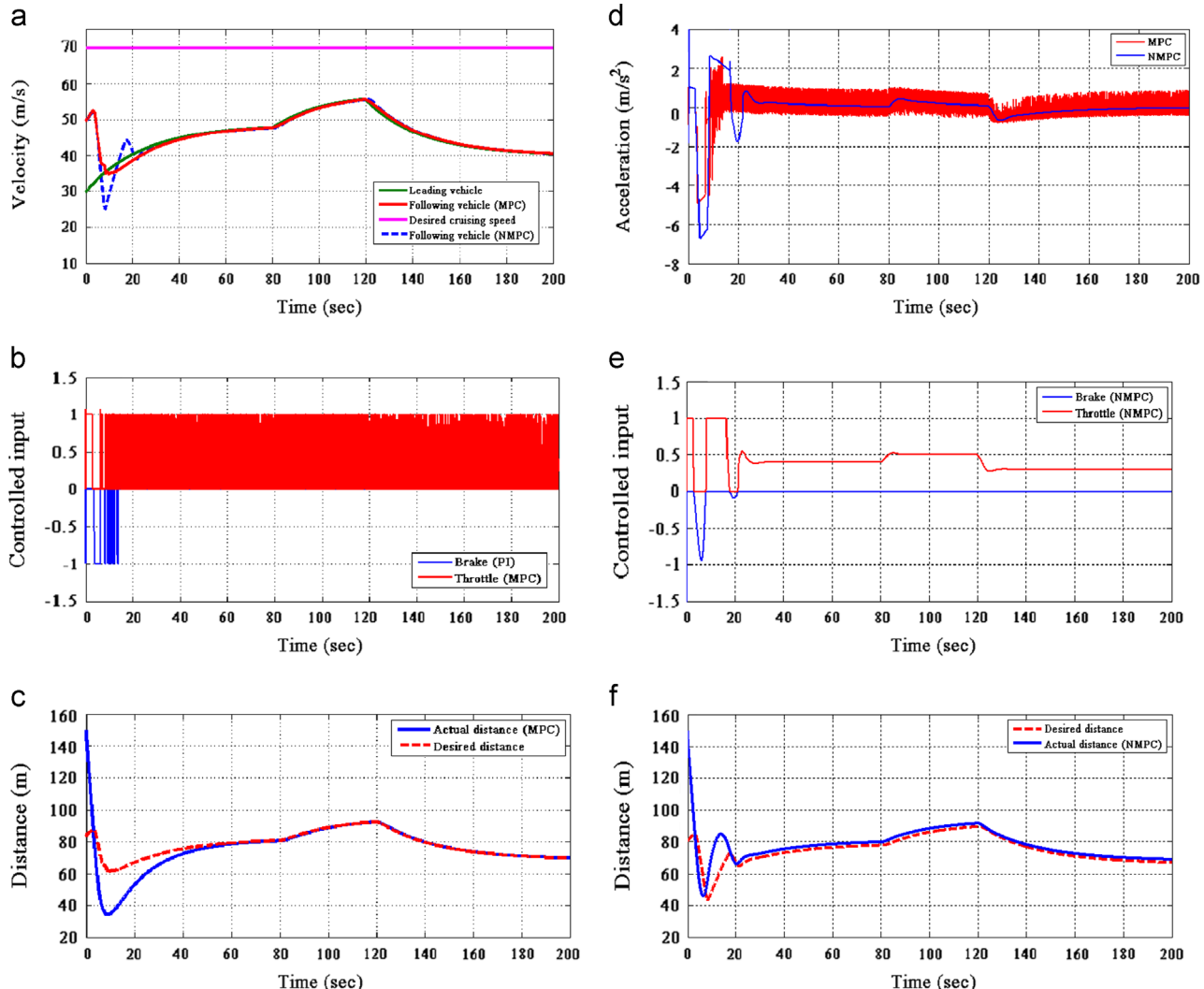


Fig. 9. The system operates in ACC mode – third set of results – r_w has been increased and dead-zone introduced, (a) velocity: leading vehicle, desired cruising speed, the actual speed when using MPC and the actual speed when using NMPC, (b) throttle and brake signals for MPC case-brake is controlled by PI controller, while throttle by MPC, (c) distance between vehicles when using MPC algorithm, (d) the acceleration of the vehicle – the results of two controllers are compared, (e) throttle and brake signals – both brake and throttle are controlled by a single NMPC, and (f) distance between vehicles when using NMPC algorithm.

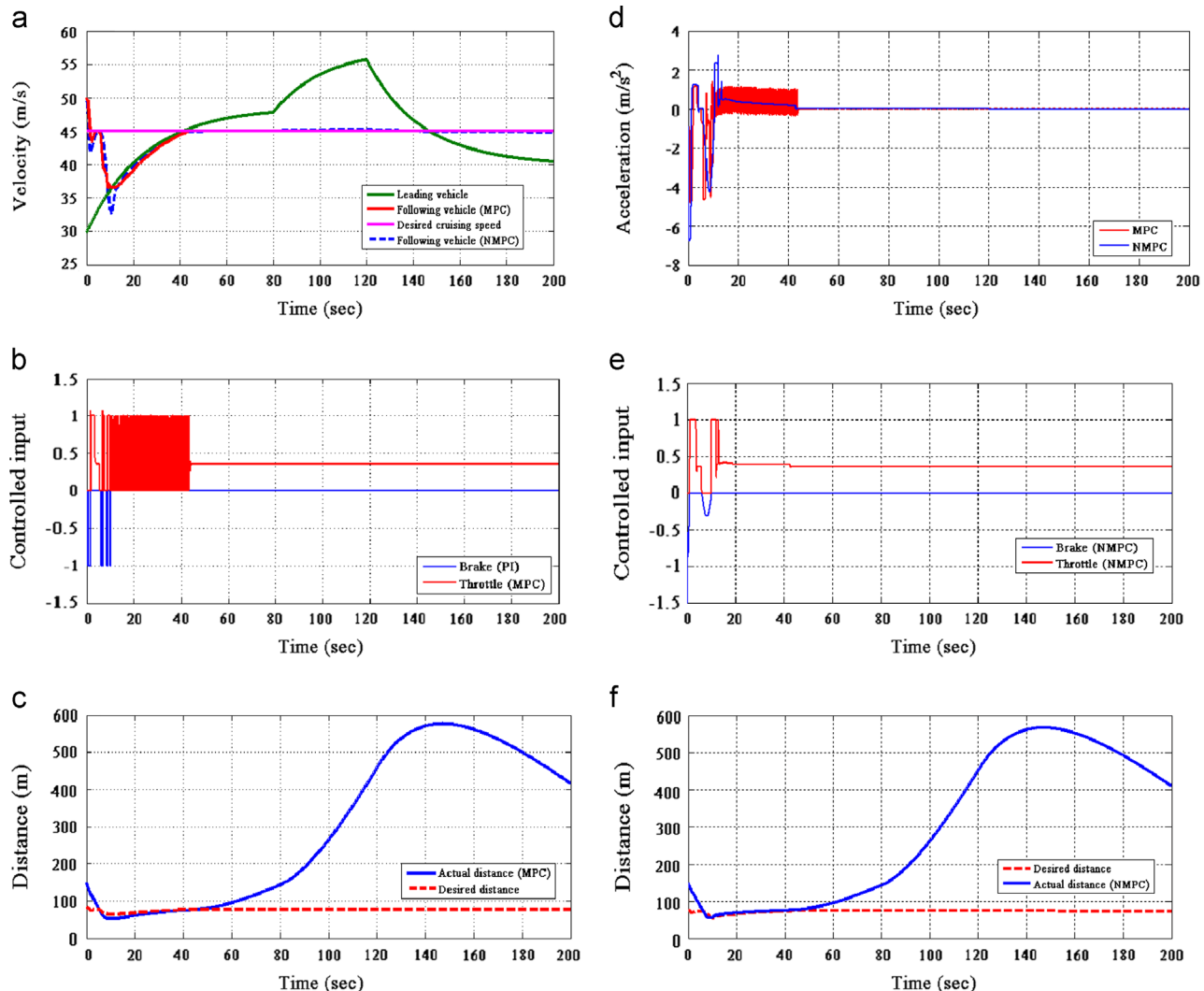


Fig. 10. The system operates in switching modes-between ACC and CC modes, (a) velocity: leading vehicle, following vehicle, desired cruising speed, the actual speed when using MPC and the actual speed when using NMPC, (b) throttle and brake signals for MPC case-brake is controlled by PI controller, while throttle by MPC, (c) distance between vehicles when using MPC algorithm, (d) the acceleration of the vehicle – the results of two controllers are compared, (e) throttle and brake signals – both brake and throttle are controlled by a single NMPC, and (f) distance between vehicles when using NMPC algorithm.

reasons; firstly, having to switch between different controllers: throttle opening through MPC and brake position by PI; secondly, the disturbance caused by the outer loop controller, e.g. switching between ACC & CC modes, affects the performance of the inner-loop controller. In case on NMPC, although there are two models used for throttle and brake operation respectively, switching between the models can be achieved smoothly. A contributing factor here is that, according to the problem formulation (28), the parameters of both models will be utilised in generating the control action at any moment in time.

In Fig. 10a the system operates initially in ACC mode and try to maintain the vehicle within the desired distance from the leading vehicle (Fig. 10b), this occurs until approximately 40 s, from this point onward the system switches to CC mode as the leading vehicle raises its speed to the value higher than desired cruise control speed (Fig. 10a). The distance tracking is fulfilled during operating the system at ACC mode. While switching the system into CC, the distance between vehicles increases. Fig. 10d illustrates smooth acceleration of the vehicle during this transition between ACC and CC modes.

Fig. 11 illustrates the simulation results for the stop & go condition. In this condition leading vehicle initially increase its

speed to around 48 m/s, and then slows down from 100 s until getting to standstill. Leading vehicle remains at standstill until 200 s, and then restarts increasing the speed. The initial distance between vehicle and the following vehicle's velocity are initially set up at 150 m and 25 m/s, respectively. The CC speed is higher than leading vehicle speed. As long as, the following vehicle is travelling far away from leading vehicle, i.e. real distance is greater than desired distance, it increases its speed to desired cruising speed. Once the distance between the two vehicles has reached the desired value, the follower vehicle starts following the leading vehicle (Fig. 11f) within the desired distance. As the leading vehicle slows down to standstill, the ACC system instantaneously functions to avoid the rear-end collision and to maintain the desired distance between vehicles. The desired distance is a function of the velocity of the following vehicle; therefore the desired distance becomes shorter as the velocity reduces. The distance between vehicles at standstill is 6 m which is the minimum distance defined so as to avoid rear-end collision. Eventually the following vehicle re-starts and increases the speed from standstill to a higher speed such that the desired distance is retained. In the vehicles with automatic transmission, when the engine runs at the idle speed i.e. the throttle pedal is not applied, a small amount of

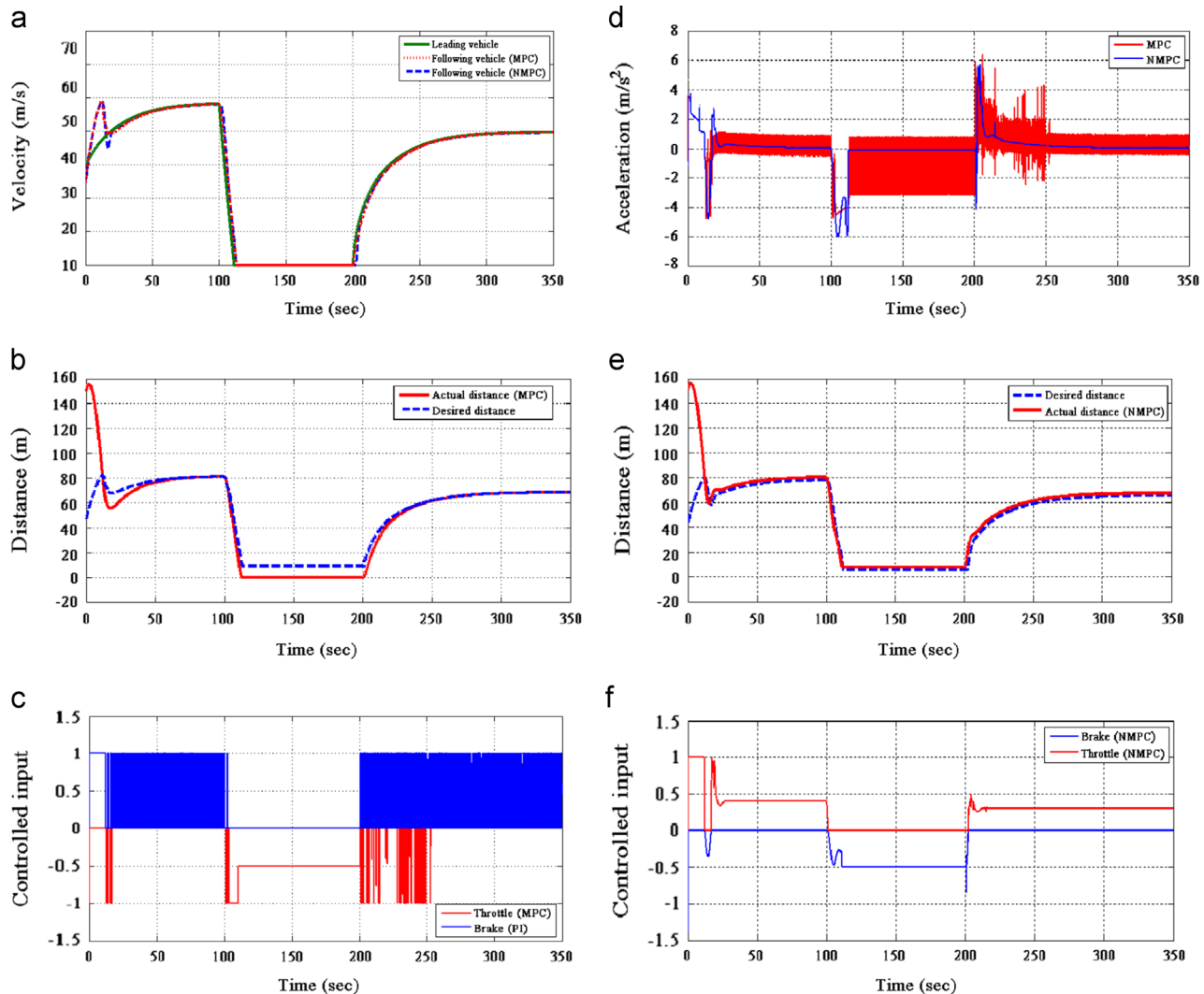


Fig. 11. The system operates in stop & go condition, (a) velocity: leading vehicle, following vehicle, desired cruising speed, the actual speed when using MPC, the actual speed when using NMPC, (b) throttle and brake signals for MPC case-brake is controlled by PI controller, while throttle by MPC, (c) distance between vehicles when using MPC algorithm, (d) the acceleration of the vehicle – the results of two controllers are compared, (e) throttle and brake signals – both brake and throttle are controlled by a single NMPC, and (f) distance between vehicles when using NMPC algorithm.

torque is transmitted through torque converter, therefore the brake needs to be applied to prevent the vehicle from moving. In the simulation model a similar condition is virtually created by imposing the lower limit of 600 rpm on the engine speed which produces 2.5 m/s velocity when the brake and the throttle position are zero. In order to avoid any unstable behaviour, the controller is configured such that at the velocity lower than 2.5 m/s the brake controlling signal $u_b=0.5$ is applied to the system instead of the value calculated value by NLMPC and subsequently the throttle controlling signal $u_t=0$. Therefore at standstill the brake controlling signal is not zero as depicted in Fig. 11c-each time instance between 110 and 200 s. As the velocity cannot be negative in the simulation, it has to be constrained: $v_h \geq 0$. The ACC system designed by utilising a single NMPC provides small variations in vehicle's acceleration (Fig. 11d). The results obtained by using NMPC have been compared with the different ACC which uses MPC. The rear-end collision can potentially occur by using MPC (Fig. 11a) and the results shows the actual distance between leader and follower approaches zero at time instances between 110 and 200 s.

The robustness of NMPC controller is tested by introducing the modelling inaccuracies, which result from changing some parameters in the nonlinear vehicle model, while using the same

controller designed previously, and without retuning. These changes are as follows:

Engine dynamics: the engine torque has been reduced to 0.8 of its original value, and also the lumped inertia of the engine and torque converter I_{el} has been changed to 0.15 kgm^2 . Those represent the smaller engine size than that used in designing the controller.

Braking dynamics: the pressure gain K_c and the lumped lag τ_b defined in Table 1 have been reduced to 0.5 and 0.1 s, respectively.

The same scenario as the one defined in Fig. 9 has been used to test the ACC system against the modelling inaccuracies. As the results demonstrate (Fig. 12), the controller provides robust control and can provide satisfactory control performance in the presence of significant inaccuracy in both the engine and brake dynamics. The comparison between the results presented in Fig. 9 and Fig. 12 shows, larger throttle and brake control efforts (Fig. 12b) are needed to follow the leading vehicle within the desired distance by utilising a different vehicle model, which its engine and braking dynamics have been changed.

The distance error (see, Fig. 12e) has demonstrated small deviations between actual and desired distances during distance tracking mode.

According to Moon et al. (2009), the ACC systems being an important part of the Advanced Driver Assistance Systems (ADAS)

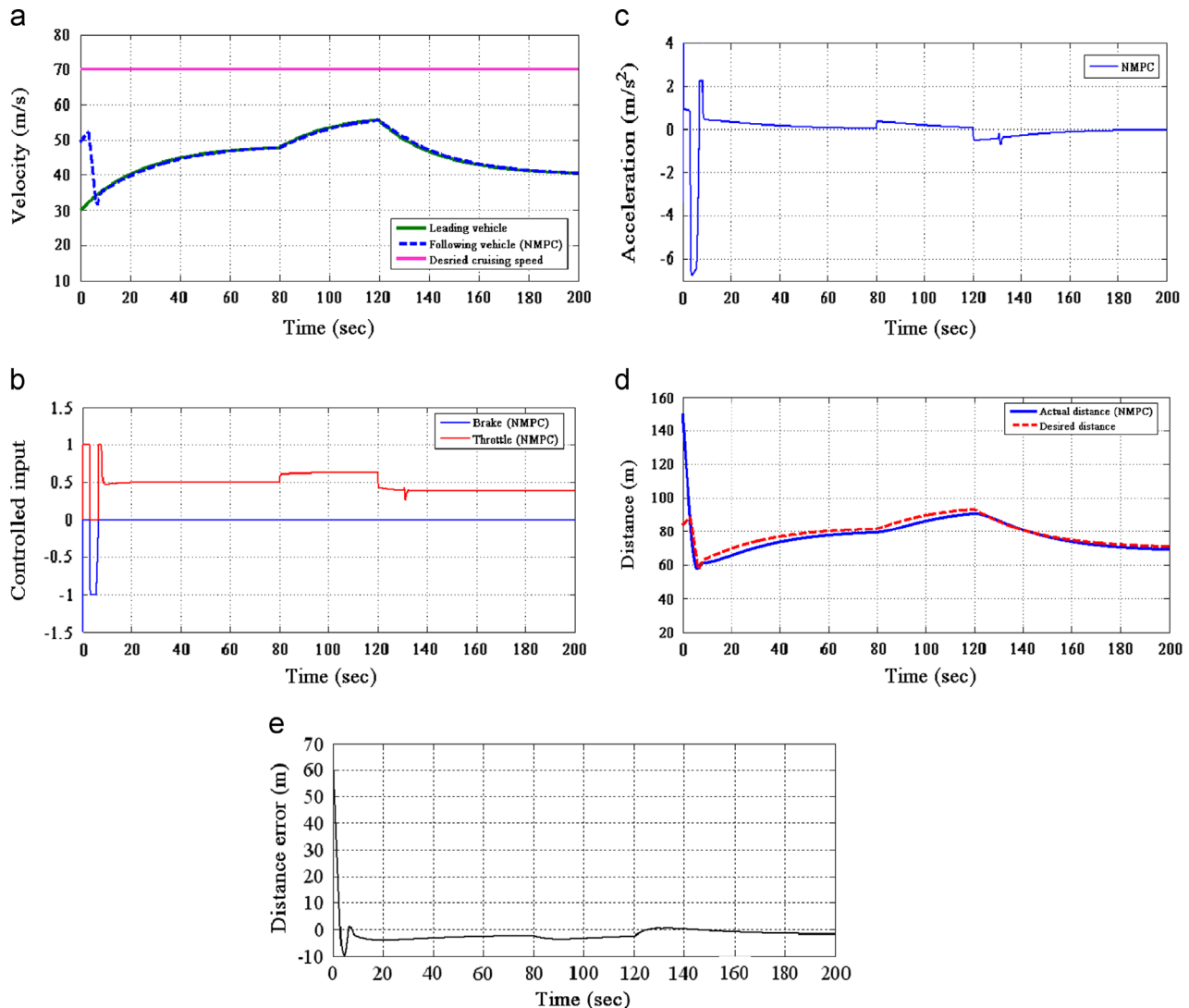


Fig. 12. The system operates in ACC mode – using a different vehicle model than used for the control design, (a) velocity: leading vehicle, following vehicle, desired cruising speed and the actual speed when using NMPC, (b) throttle and brake signals – both brake and throttle are controlled by a single NMPC, (c) the acceleration of the vehicle, (d) distance between the vehicles, and (e) distance tracking error.

are also designed to enhance the comfort for the driver and the passengers. They feel comfortable if the vehicle acceleration varies approximately within the range of -3 and 3 m/s^2 . In the normal conditions, the coordinated operation between the brake and the throttle is very important for achieving driving comfort. The results obtained through the simulations have demonstrated that the acceleration magnitudes are retained within the comfortable range during tracking. Furthermore, the proposed method based on NMPC could enhance the coordination between the brake and throttle operations during the function of the ACC system, resulting in more comfortable driving. (Of course, to avoid the collision and to ensure the safety, when the vehicle travelling ahead (leading vehicle) suddenly stops, severe braking may be required.)

5. Conclusions

In this paper, the design procedures for an ACC system based on one control layer covering both the ACC&CC modes by utilising a single NMPC has been explained. NMPC equation used in this paper is developed based on state-dependent representation of

linear models corresponding to the modes of the operation: accelerating-throttle is active, and braking-brake is active. The state of the system-containing only the state of the following vehicle-were augmented by adding the state of the leading vehicle. The reference trajectories for ACC&CC modes were presented including prediction of the vehicle speed, the desired tracking distance, the desired cruising speed, the prediction of the tracking distance between the vehicles, and the prediction of the relative velocity. Furthermore, an algorithm based on changing the reference trajectories were provided in order to implement automated switching between CC and ACC through utilising a single NMPC. The method proposed in this paper has aimed at eliminating the need of designing the two separate control loops for regulating the brake and throttle opening. Furthermore, the distance tracking objective was incorporated into the design of NMPC providing the smooth performance in distance and speed tracking. The ACC system based on the proposed method has been developed in MATLAB/SIMULINK® and some results by introducing various traffic scenarios have been obtained. The presented results by simulation establish a good and flawless performance of the system. Also, the results of the proposed method have been

compared to other approach which was devised based on the outer loop and inner loop controllers. The comparison proves that the proposed method provides considerably better functionality in term of not only the distance and the speed tracking but also the vehicle acceleration resulting from smooth variations of the brake and throttle opening.

For the future work, the prediction of the switching sequence will be incorporated into the ACC algorithm. Additionally, the algorithm can be further developed, to include the gear shifting as a control decision for optimisation purposes.

The approach to control design in this paper includes approximation of the real, non-linear system by piecewise affine models. An open research question is analysis of feasibility and robustness of the non-linear system. Concerning the feasibility, this will start playing important role when the hard constraints on the states (e.g. maximum engine rpm) and inputs (e.g. maximum braking torque) are combined with soft constraints on outputs (e.g. minimum distance between vehicles). Future work may therefore include the analysis of reachable sets of states. With affine constraints, the polyhedral sets seem to be the most appropriate option. Concerning the robustness, some initial simulations, presented in this paper, suggest that the algorithms are quite robust with respect to the error made by linear parameterisation of the models. The approach presented here can be further extended by including more linearised models. In [Shakouri et al. \(2011\)](#) the authors considered 10 linearised models for the “accelerating” part. This has provided higher accuracy of the modelling part. Including more linearised models is possible, within the same algorithm, as developed in this paper. Furthermore, stabilisable sets can be computed in a fashion similar to the feasibility analysis.

Finally, note that, according to [Bemporad, Ferrari-Trecante, and Morari \(2000\)](#), the hybrid control systems can be described equivalently by piecewise affine models (used in this paper) and by Mixed Logical Dynamic (MLD) models. This means that, for instance, the feasibility conditions obtained from the two approaches will be identical. Nevertheless, it may be interesting to compare the computational effort, ease of design and robustness when using the two approaches.

Acknowledgements

The authors would like to thank the industrial collaborators for discussions concerning practical aspects of operation of the automotive power train:

- Peter Kock from the Central Engineering Division of MAN (Truck & Bus) Nutzfahrzeuge AG in Munich, Germany,
- Paul Darnell from Jaguar-Land Rover.

Appendix A. The numerical values of the various state-space equations

Coefficients of the state-space equations in continuous-time:

$$A_{t(\text{cont})} = \begin{bmatrix} -5 & 0 & 0 \\ -0.7844 & -0.0626 & 0.001034 \\ 0 & 210.7778 & -5.016 \end{bmatrix}, B_{t(\text{cont})} = \begin{bmatrix} 0 \\ 0 \\ 29650 \end{bmatrix}$$

$$A_{b(\text{cont})} = \begin{bmatrix} -55 & 0 & 0 \\ -15.684 & -0.01262 & 0 \\ 0 & 0 & -50 \end{bmatrix}, B_{b(\text{cont})} = \begin{bmatrix} 150 \\ 0 \\ 0 \end{bmatrix}$$

Appendix B

Coefficients of the augmented state-space equations in continuous-time:

$$A_{t(\text{augc})} = \begin{bmatrix} -5 & 0 & 0 & 0 & 0 \\ -0.7844 & -0.0626 & 0.001034 & 0 & 0 \\ 0 & 210.7778 & -5.016 & 0 & 0 \\ 0 & 0 & 0 & 0 & 0 \\ 0 & -1 & 0 & 1 & 0 \end{bmatrix},$$

$$B_{t(\text{augc})} = \begin{bmatrix} 0 \\ 0 \\ 29650 \\ 0 \\ 0 \end{bmatrix}$$

$$A_{b(\text{augc})} = \begin{bmatrix} -55 & 0 & 0 & 0 & 0 \\ -15.684 & -0.01262 & 0 & 0 & 0 \\ 0 & 0 & -50 & 0 & 0 \\ 0 & 0 & 0 & 0 & 0 \\ 0 & -1 & 0 & 1 & 0 \end{bmatrix},$$

$$B_{b(\text{augc})} = \begin{bmatrix} -150 \\ 0 \\ 0 \\ 0 \\ 0 \end{bmatrix}$$

Appendix C

Coefficients of the augmented state-space equations in discrete-time:

$$A_{t(\text{augd})} = \begin{bmatrix} 0.9512 & 0 & 0 & 0 & 0 \\ -0.0076 & 0.9994 & 0.0000 & 0 & 0 \\ -0.0080 & 2.0551 & 0.9511 & 0 & 0 \\ 0 & 0 & 0 & 1.0000 & 0 \\ 0.0000 & -0.0010 & -0.0000 & 0.0100 & 1.0000 \end{bmatrix},$$

$$B_{t(\text{augd})} = \begin{bmatrix} 0.0000 \\ 0.00150 \\ 2989.1876 \\ 0 \\ -0.0000 \end{bmatrix}$$

$$A_{b(\text{augd})} = \begin{bmatrix} 0.5769 & 0 & 0 & 0 & 0 \\ -0.1206 & 0.9999 & 0 & 0 & 0 \\ 0 & 0 & 0.6065 & 0 & 0 \\ 0 & 0 & 0 & 1.0000 & 0 \\ 0.0007 & -0.0100 & -0.0000 & 0.0100 & 1.0000 \end{bmatrix},$$

$$B_{b(\text{augd})} = \begin{bmatrix} -1.1538 \\ 0.0987 \\ 0 \\ 0 \\ 0.0003 \end{bmatrix}$$

Appendix D

Coefficients of the incremental state-space equations in discrete-time:

$$A_{t,1} = \begin{bmatrix} 0.9512 & 0 & 0 & 0 & 0 & 0 \\ -0.0076 & 0.9994 & 0.0000 & 0 & 0 & 0 \\ -0.0080 & 2.0551 & 0.9511 & 0 & 0 & 0 \\ 0 & 0 & 0 & 1.0000 & 0 & 0 \\ 0.0000 & -0.0100 & -0.0000 & 0.0100 & 1.0000 & 0 \\ -0.0076 & 0.9994 & 0.0000 & 0 & 0 & 1.0000 \end{bmatrix}, B_{t,1} = \begin{bmatrix} 0 \\ 0.0015 \\ 289.1876 \\ 0 \\ -0.0000 \\ 0.0015 \end{bmatrix}$$

$$A_{t,2} = \begin{bmatrix} 0.9512 & 0 & 0 & 0 & 0 & 0 \\ -0.0076 & 0.9994 & 0.0000 & 0 & 0 & 0 \\ -0.0080 & 2.0551 & 0.9511 & 0 & 0 & 0 \\ 0 & 0 & 0 & 1.0000 & 0 & 0 \\ 0.0000 & -0.0100 & -0.0000 & 0.0100 & 1.0000 & 0 \\ 0.0000 & -0.0100 & -0.0000 & 0.0100 & 1.0000 & 1.0000 \end{bmatrix}, B_{t,2} = \begin{bmatrix} 0 \\ 0.0015 \\ 289.1876 \\ 0 \\ -0.0000 \\ -0.0000 \end{bmatrix}$$

$$A_{t,3} = \begin{bmatrix} 0.9512 & 0 & 0 & 0 & 0 & 0 \\ -0.0076 & 0.9994 & 0.0000 & 0 & 0 & 0 \\ -0.0080 & 2.0551 & 0.9511 & 0 & 0 & 0 \\ 0 & 0 & 0 & 1.0000 & 0 & 0 \\ 0.0000 & -0.0100 & -0.0000 & 0.0100 & 1.0000 & 0 \\ 0.0076 & -0.9994 & -0.0000 & 1.0000 & 0 & 1.0000 \end{bmatrix}, B_{t,3} = \begin{bmatrix} 0 \\ 0.0015 \\ 289.1876 \\ 0 \\ -0.0000 \\ -0.0015 \end{bmatrix}$$

$$A_{b,1} = \begin{bmatrix} 0.5769 & 0 & 0 & 0 & 0 & 0 \\ -0.1206 & 0.9999 & 0 & 0 & 0 & 0 \\ 0 & 0 & 0.6065 & 0 & 0 & 0 \\ 0 & 0 & 0 & 1.0000 & 0 & 0 \\ 0.0007 & -0.0100 & 0 & 0.0100 & 1.0000 & 0 \\ -0.1206 & 0.9999 & 0.0000 & 0 & 0 & 1.0000 \end{bmatrix}, B_{b,1} = \begin{bmatrix} -1.1538 \\ 0.0987 \\ 0 \\ 0 \\ -0.0003 \\ 0.0987 \end{bmatrix}$$

$$A_{b,2} = \begin{bmatrix} 0.5769 & 0 & 0 & 0 & 0 & 0 \\ -0.1206 & 0.9999 & 0 & 0 & 0 & 0 \\ 0 & 0 & 0.6065 & 0 & 0 & 0 \\ 0 & 0 & 0 & 1.0000 & 0 & 0 \\ 0.0007 & -0.0100 & 0 & 0.0100 & 1.0000 & 0 \\ 0.0007 & -0.0100 & 0 & 0.0100 & 1.0000 & 0 \end{bmatrix}, B_{b,2} = \begin{bmatrix} -1.1538 \\ 0.0987 \\ 0 \\ 0 \\ -0.0003 \\ -0.0003 \end{bmatrix}$$

$$A_{b,3} = \begin{bmatrix} 0.5769 & 0 & 0 & 0 & 0 & 0 \\ -0.1206 & 0.9999 & 0 & 0 & 0 & 0 \\ 0 & 0 & 0.6065 & 0 & 0 & 0 \\ 0 & 0 & 0 & 1.0000 & 0 & 0 \\ 0.0007 & -0.0100 & 0 & 0.0100 & 1.0000 & 0 \\ 0.1206 & -0.9999 & 0 & 1.0000 & 0 & 1.0000 \end{bmatrix}, B_{b,3} = \begin{bmatrix} -1.1538 \\ 0.0987 \\ 0 \\ 0 \\ -0.0003 \\ -0.0987 \end{bmatrix}$$

$$C = [0 \ 0 \ 0 \ 0 \ 0 \ 1]$$

References

- Axehill, D., & Sjöberg J. (2003). *Adaptive cruise control for heavy vehicles: Hybrid control and MPCA* (Student thesis). Department of Electrical Engineering, Linköping University.
- Bemporad, A., Ferrari-Trecante, G., & Morari, M. (2000). Observability and controllability of piecewise affine and hybrid systems. *IEEE Transactions on Automatic Control*, 1864–1876.
- Desjardins, C., & Chaib-draa, B. (2011). Cooperative adaptive cruise control; a reinforcement: A reinforcement learning approach. *IEEE Transactions on Intelligent Transportation System*, 12(4), 1248–1260.
- Dutka, A. S., Ordys A. W., & Grimble M. J. (2005). Optimized discrete-time state dependent riccati equation regulator. In *Proceedings of the American control conference*. Portland, OR, USA.
- Eidehall, A., Pohl, J., & Gustafsson, F. (2007). Joint road geometry estimation and vehicle tracking. *Control Engineering Practice*, 15, 1484–1494.
- Gerdes, J. C., & Hedrick, J. K. (1997). Vehicle speed and spacing control via coordinated throttle and brake actuation. *Control Engineering Practice*, 5, 1607–1614.
- Hellström, E., Ivarsson, M., Åslund, J., & Nielsen, L. (2009). Look-ahead control for heavy truck to minimize trip time and fuel consumption. *Control Engineering Practice*, 17, 245–254.
- Isermann, R., Mannale, R., & Schmitt, K. (2012). Collision-avoidance systems PRORETA: Situation analysis and intervention control. *Control Engineering Practice*, 20, 1236–1246.
- Jonsson, J. (2003). *Fuel optimized predictive following in low speed condition* (Master's thesis). Linköpings University.

- Keulen, T., Naus, G., Jagar, B., Molengraft, R., Steinbuch, M., & Aneke, E. (2009). Predictive cruise control in hybrid electric vehicles. *World Electric Vehicle Journal*, 3, 1–11.
- Kouvaritakis, B., Canon, M., & Rossiter, J. A. (1999). Nonlinear model based predictive control. *International Journal of Control*, 72, 919–928.
- Kozica, E. (2005). Look ahead cruise control: road slope estimation and control sensitivity (Master's degree Project). Stockholm, Sweden.
- Lattemann, F., Neiss, K., Terwen, S., & Connolly, T. (2004). The Predictive cruise control-a system to reduce fuel consumption of heavy duty trucks. SAE World Congress. Detroit, MI, USA: SAE Technical Paper Series.
- Liuping, W. (2009). *Model predictive control system design and implementation using matlab* (2nd ed.). Springer.
- Majdoub, E. L., Giri, K. F., Ouadi, H., Dugard, L., & Chaoui, F. Z. (2012). Vehicle longitudinal motion modelling for nonlinear control. *Control Engineering Practice*, 20, 69–81.
- Martinez, J. J., & Canudas-de-Wit, C. (2007). A safe longitudinal control for adaptive cruise control and stop-and-go scenarios. *IEEE Transactions on Control Systems Technology*, 15, 473–479.
- Moon, S., Moon, I., & Yi, K. (2009). Design, tuning and evaluation of a full-range adaptive cruise control system with collision avoidance. *Engineering Control Practice*, 17, 442–455.
- Park, S., Hwang, J. P., & Kang, H. J. (2010). Vehicle tracking using a microwave radar for situation awareness. *Control Engineering Practice*, 18, 383–395.
- Ploeg, J., Serrarens, A. F. A., & Heijenk, G. J. (2011). Connect and drive: Design and evaluation of cooperative adaptive cruise control for congestion reduction. *Journal of Modern Transportation*, 19(9), 207–213.
- Riis, P. (2007). *Adaptive cruise controller simulation as an embedded distributed system* (M.Sc. thesis). Linkoping University.
- Ruszczynski, Andrzej (2006). *Nonlinear optimisation*. Princeton, NJ: Princeton University Press978-0691119151.
- Shakouri, P. (2012). *Designing of the adaptive cruise control system-switching controller* (Ph.D. thesis). UK: Kingston University of London.
- Shakouri, P., Ordys A., Laila D. S., & Askari M. R. (2011). Adaptive cruise control system: comparing gain-scheduling PI and LQ controllers. In *18th IFAC World Congress*. Milano, Italy.
- Shakouri, P., Ordys, A., Askari, M., & Laila, D. S. (2010). Longitudinal vehicle dynamics using Simulink/Matlab. In *Proceedings of the UKACC international conference on CONTROL*. Coventry.
- Shladover, S. E., et al. (2009). Effects of cooperative adaptive cruise control on traffic flow: testing drivers' choices of following distances. California PATH Research Report, California Path Programme, Institute of Transportation Studies, University of California, Berkeley.
- Short, M., Pont M. J., & Huang Q.. (2004). *Simulation of vehicle longitudinal dynamic*. Embedded System Laboratory University of Leicester, safety and reliability of Distributed Embedded Systems, Leicester.
- Naus, G. J. L., Ploeg, J., van de Molengraft, M. J. G., Heemels, W. P. M. H., & Steinbuch, M. (2010). Design and implementation of parameterized adaptive cruise control: An explicit model predictive control approach. *Control Engineering Practice*, 18(8), 882–892.
- Vahidi, A., & Eskandarian A.. (2003). Vehicle dynamic simulation with coupled multibody and finite element models. *Research Advances in Intelligent Collision Avoidance and Adaptive Cruise Control* (IEEE Trans. Intelligent Transportation system).
- van den Bleek, R. A. P. M. (2007). *Design of a hybrid adaptive cruise control stop-&-go system* (Master's thesis). TNO Science & Industry, Technische Universiteit Eindhoven.
- ven Arem, B., ven Driel, C. J. G., & Visser, R. (2006). The impact of cooperative adaptive cruise control on traffic-flow characteristics. *IEEE Transportation on Intelligent Transportation Systems*, 7(4), 429–436.
- Wang, J. Y. (2001). *Theory of ground vehicle* (3rd ed.). Wiley Inter Science.
- Wingren, A. (2005). *Fordonsreglering med framförhållning*. Vehicular System (M.Sc. thesis). Department of Electrical Engineering, Linköping University.
- Winner, H., Winter, K., Lucas, B., et al. (2003). ACC adaptive cruise control, the bosch yellow jacket.
- Xiao, Lingyun, & Gao, Feng (2010). A comprehensive review of the development of adaptive cruise control system. *Vehicle System Dynamics*, 48(10), 1167–1192.
- Youssef, A. M., Ordys, A. W., & Grimble, M. J. (2004). Nonlinear predictive control for fast constrained systems. In *Proceedings of the IEEE conference on methods and models in automation and robotics*. Miedzyzdroje, Poland.
- Zhou, W., & Zhang, S. (2003). Analysis of distance headways. In *Proceedings of the Eastern Asia society for transportation studies*.